The Analysis of Visual Motion: A Comparison of Neuronal and Psychophysical Performance

Kenneth H. Britten,[1] Michael N. Shadlen,[1] William T. Newsome,[1] and J. Anthony Movshon[2]

[1]Department of Neurobiology, Stanford University School of Medicine, Stanford, California 94305 and [2]Howard Hughes Medical Institute, Center for Neural Science, and Department of Psychology, New York University, New York, New York 10003

We compared the ability of psychophysical observers and single cortical neurons to discriminate weak motion signals in a stochastic visual display. All data were obtained from rhesus monkeys trained to perform a direction discrimination task near psychophysical threshold. The conditions for such a comparison were ideal in that both psychophysical and physiological data were obtained in the same animals, on the same sets of trials, and using the same visual display. In addition, the psychophysical task was tailored in each experiment to the physiological properties of the neuron under study; the visual display was matched to each neuron's preference for size, speed, and direction of motion. Under these conditions, the sensitivity of most MT neurons was very similar to the psychophysical sensitivity of the animal observers. In fact, the responses of single neurons typically provided a satisfactory account of both absolute psychophysical threshold and the shape of the psychometric function relating performance to the strength of the motion signal. Thus, psychophysical decisions in our task are likely to be based upon a relatively small number of neural signals. These signals could be carried by a small number of neurons if the responses of the pooled neurons are statistically independent. Alternatively, the signals may be carried by a much larger pool of neurons if their responses are partially intercorrelated.

How is the exquisite psychophysical sensitivity of human and animal observers related to the sensitivity of individual cortical neurons? While there can be little doubt that such a relationship exists, the nature of the transformation between sensory signals and perceptual responses remains the uncertain province of theory rather than experiment. A fundamental problem is to estimate the size and location of the pool of neurons that contributes to any particular perceptual judgement. The traditional *trigger feature* concept in sensory physiology (Lettvin et al., 1959; Barlow, 1972) attributes to each neuron a unique role in

signaling the presence of a particular feature in the visual environment. "Fuzzy" versions of the trigger feature hypothesis, while less emphatic about the impact of individual neurons, continue to focus upon the signaling capacities inherent in the activity of a relatively small population of neurons.

In contrast, more recent psychological approaches have tended to emphasize the role of larger neuronal networks and pools in solving even simple perceptual problems. Unfortunately, current pooling models lead to widely divergent expectations concerning the relationship between neuronal and psychophysical sensitivities to visual stimuli. Consider, for example, an observer attempting to discriminate a weak signal within a noisy visual display. Because of the variety of stimulus selectivities evident among neurons, some of the signals available within the visual cortex will carry little or no information about the particular stimulus being viewed. If the neuronal machinery that forms the perceptual judgement is influenced by neurons that are insensitive as well as by neurons that are sensitive to the signal being discriminated, psychophysical judgements would be substantially *degraded* compared to those based only on the activity of the most sensitive neurons (e.g., Pelli, 1985). On the other hand, psychophysical judgements could actually be *improved* relative to the most sensitive neurons if noise arising within the CNS were averaged out by pooling information across a selected population of sensitive neurons (e.g., Pirenne, 1943; Tolhurst et al., 1983). Empirical evidence concerning the relative sensitivities of neurons and psychophysical observers is therefore critical to our understanding of the mechanisms by which neural activity in the cerebral cortex mediates perceptual decisions.

The idea of relating central neuronal activity to sensory experience was first explored in a quantitative fashion by Werner and Mountcastle (1963), who enunciated some fundamental principles for the analysis of neuronal discharge in a psychophysical context. More recently, the relationship between the sensitivity of visual cortical neurons and psychophysical judgement has been actively investigated by several laboratories. Psychophysical and neuronal performance has been compared in the domains of contrast sensitivity, orientation sensitivity, spatial frequency sensitivity, position (or phase) sensitivity, and acuity (Tolhurst et al., 1983; Parker and Hawken, 1985; Barlow et al., 1987; Bradley et al., 1987; Hawken and Parker, 1990; Vogels and Orban, 1990; Zohary, 1992). The general finding of these studies was that the sensitivities of most cortical neurons fell considerably short of psychophysical sensitivity. Typically, only the "best" neurons yielded performance that approached psychophysical levels. Most of these studies were limited, how-

ever, in that the comparison between psychophysical and neural performance was based on data obtained at different times, under different conditions, and often in different species.

We have now compared the capacity of single cortical neurons for signaling motion direction with the capacity of trained rhesus monkeys to discriminate motion direction psychophysically. We felt that this comparison would be most incisive if the neuronal and psychophysical performance were measured simultaneously in the same animal, and in the context of a discrimination task well matched to the physiological properties of the neuron being studied. We therefore recorded the responses of directionally selective neurons while rhesus monkeys discriminated the direction of near-threshold motion signals in a stochastic visual display. For each neuron, the visual discriminanda were adjusted to match the preferences of the neuron under study, so that the physiological and psychophysical data sets were obtained under conditions in which the neuron's activity was most likely to be relevant to the animal's perceptual decision. The physiological recordings were carried out in visual area MT (V5), an extrastriate area that contains a preponderance of directionally selective neurons (Dubner and Zeki, 1971; Zeki, 1974). We have shown previously that neural activity in MT contributes importantly to psychophysical performance on our direction discrimination task (Newsome and Pare, 1988; Salzman et al., 1990, 1992).

In contrast to previous studies, our results reveal that the discriminative capacities of most MT neurons are remarkably similar to the discriminative capacity of the seeing animal. The responses of single neurons can account not only for the absolute psychophysical threshold in a motion discrimination task, but also for the shape of the psychometric function that relates stimulus strength to visual performance. The results suggest that perceptual judgements in our psychophysical task are based on a relatively small number of independent neural signals present in the responses of MT neurons. The size of the neuronal pool carrying these signals is likely to depend critically upon the degree of intercorrelated firing among the pooled cells.

We have briefly described some of these results elsewhere (Newsome et al., 1989a, 1990).

Materials and Methods

Subjects, surgery, and daily routine

Three adult rhesus macaques (*Macaca mulatta*, two male and one female) were used in this study. Prior to recording, a stainless steel device for stabilizing head position was surgically attached to the skull (Evarts, 1966), and a scleral search coil for measuring eye movements was implanted around one eye (Judge et al., 1980). Following several months of training on a direction discrimination task, a stainless steel cylinder was surgically implanted over occipital cortex, allowing a posterior electrode approach for electrophysiological recording in MT. Surgical procedures were performed under aseptic conditions using either barbiturate or halothane anesthesia. Following recovery from surgery, the monkeys began daily training or recording sessions that lasted from 2 to 6 hr. Each animal was comfortably seated in a primate chair with its head restrained during recording sessions, and was returned to its home cage following the session. The animal's fluid intake was restricted during recording or training, and behavioral control was achieved using operant conditioning techniques, with water or juice as a positive reward. All procedures conformed to guidelines established by the NIH for the care and use of laboratory animals.

Random dot stimuli

We used a visual display designed to isolate motion-sensitive mechanisms by providing a controlled motion signal whose strength did not alter the average spatial or temporal structure of the stimulus; this
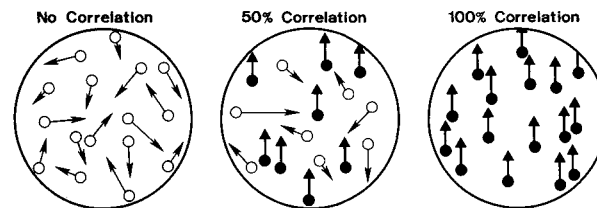

Figure 1. A schematic diagram of the stochastic motion stimulus employed in this study. Each stimulus was composed of a stream of randomly positioned dots plotted on a CRT monitor. The strength of the motion signal in the display was determined by the amount of "correlation" introduced as the dots were plotted. The *left panel*, for example, illustrates the 0% correlation state in which each dot position was chosen completely at random. This stimulus comprised "white noise" in the motion domain since all directions and speeds were equally present in the display. The *center panel* depicts the 50% correlation state in which half of the dots were positioned randomly ("noise" dots) while the remaining half were plotted with a fixed spatial and temporal offset with respect to previously plotted dots ("signal" dots). In this version of the display, a unidirectional motion signal coexisted with a masking motion noise. The *right panel* shows the 100% correlated state in which each dot carried an identical motion signal. This version of the display contained the strongest motion signal that could be presented with our set of stimuli.

display is similar in concept to one used by Morgan and Ward (1980). The display was created on a large-screen CRT monitor (Hewlett-Packard 1321B or XYtron A21-63; P4 phosphor, 0.2 cd/m² mean luminance) by a PDP11 computer that plotted a rapid sequential stream of bright dots, each 0.1° in diameter. In the absence of a coherent motion signal, the position of each dot was random, and the display appeared to contain a fluctuating pattern of spatiotemporal white noise. Because the dots were all uncorrelated with one another, the display contained a random mixture of directions and speeds in which all spatiotemporal combinations were equally probable. We imposed a coherent motion signal by plotting a specified proportion of the dots with a specific spatiotemporal relation to previously displayed dots. Varying the spatial and temporal offset with which these "signal" dots were plotted allowed us to control the direction and speed of the coherent signal. When enough signal dots were added, the display appeared to contain a global motion flow superimposed upon the randomly fluctuating background motion. The proportion of signal dots, p, is the independent variable that controls the strength of the motion signal; we refer to this value as the *correlation*. The *speed* of the signal is determined by the ratio of the spatial and temporal offsets, $\Delta x/\Delta t$. In the present experiments, we fixed Δt at 45 msec, a near-optimal value for psychophysical performance in monkeys and humans (Morgan and Ward, 1980; Newsome and Pare, 1988); the magnitude of Δx was varied from neuron to neuron between 0.02° and 1.3° to provide speeds between 0.4 and 28.4 degrees/sec. The *density* of the dots was determined by the rate at which they were plotted and the area of the screen. In these experiments the rate was always 6.67 kHz and the unmasked area was 400 degrees², resulting in a density of 16.7 dots/degree²/sec. Psychophysical measurements in humans show that motion sensitivity is unaffected by density for a wide range around this value (Downing and Movshon, 1989).

Although each dot was plotted sequentially and was present only for the 150 μsec persistence of the P4 phosphor, the visual persistence of each dot was much longer, perhaps 100 msec, and created the impression of a display containing several hundred dots at any moment.

Under most conditions the direction of motion could not be established by inspecting the path of any particular signal dot. The probability that any dot would be renewed as a signal dot is given by the correlation p; the "lifetimes" of the dots are geometrically distributed, and the probability that a particular dot will "live" through N presentations is p^{N-1}. Thus, for correlation values less than about 0.5, few dots had a lifetime in excess of 150 msec. For values in the typical threshold range (below 0.1), the chance of any signal dot surviving more than two lives was vanishingly small. Thus, the motion content of the display could only be extracted by integrating brief local motion signals over time and space (Downing and Movshon, 1989).

Schematic drawings of this stimulus for various correlation values are shown in Figure 1. At 0% correlation, shown in Figure 1 (left), there

were no signal dots and the resulting display was pure noise, with equal amounts of motion in all directions and over a wide range of speeds. At intermediate correlation levels (Fig. 1, center), some dots carried signal while others provided noise by virtue of random pairings in space and time between noise dots. If the correlation was increased to 100% (Fig. 1, right), every dot was a signal dot, and the display was a rigidly translating random dot field with no noise.

The values used to determine the locations of the dots and to choose any particular dot as a signal dot were drawn from a pseudorandom *m*-sequence computed by special hardware using a 31-bit shift register. If the shift register was "seeded" with a particular value, it created the same sequence of values and thus the same display for any fixed choice of p, Δx, and Δt. For most experiments (160 of 216 neurons), the shift register was seeded with a different value on each trial, and the precise pattern of dots in space and time was unique for each repetition. In the remaining 56 experiments, however, this within-stimulus variance was eliminated by seeding the shift register with the same value on every trial. For 31 of these 56 neurons, data were obtained only without stimulus variance. For the other 25 neurons, trials containing stimulus variance were randomly interleaved with trials containing no stimulus variance. We found no effect of stimulus variance on any of the physiological or psychophysical measurements reported in this article, and we therefore treat the 216 neurons in our sample as a homogeneous group for the purposes of data analysis.

Electrophysiological recording

Initial mapping penetrations were made with glass-coated platinum-iridium microelectrodes with impedances between 0.5 and 1.0 MΩ (at 1 kHz). MT was identified on the basis of its characteristic location within the superior temporal sulcus, its preponderance of responsive, directionally selective neurons, and its characteristic topography. After locating MT, we secured a plastic guide tube support grid inside the recording cylinder (Crist et al., 1988). The grid permitted stainless steel guide tubes to be inserted into the cortex at 1 mm intervals across the entire recording cylinder, and single guide tubes could be left in place between experiments for multiple days of recording. A snugly fitting, antibiotic-coated pin was inserted into the guide tube between experiments to isolate the brain from the environment within the recording cylinder. Guide tubes were usually inserted to within 2–5 mm of MT, and we recorded through these guide tubes using stainless steel or tungsten microelectrodes (0.5–2 MΩ impedance at 1 kHz) insulated with varnish or Parylene (Frederick Haer Inc., Micro Probe Inc.). We increased the randomness of electrode sampling by bending each electrode slightly so that its exact path through the cortex after emerging from the guide tube varied from day to day. Using this system, we could record from single MT neurons for durations up to 3 hr, although 20–60 min was much more typical.

Behavioral control and data acquisition were accomplished using a PDP11 minicomputer running software for real-time experiments developed at the Laboratory for Sensorimotor Research of the National Eye Institute (Hays et al., 1982). The signal from the microelectrode was amplified and action potentials from single neurons were isolated using a time-amplitude window discriminator (Bak Electronics). The window discriminator produced TTL pulses corresponding to single action potentials whose times of arrival were recorded and stored by the computer. Unit activity could be monitored visually by raster displays compiled by the computer or by an audio monitor driven by the electrode signal. Eye movement signals were measured using a scleral search coil system (C-N-C Engineering) and were transmitted to the computer as x- and y-position voltages. These signals were used to enforce behavioral contingencies (see below) and to present an on-line visual display of the monkey's eye position. A second PDP11, under control of the first, was used to compute and display the random dot patterns described above.

In each daily session, we searched for single units while the monkey fixated a spot of light projected from a laser or LED light source. Typically, the search stimulus was a moving bar from a hand-held slit retinoscope or a moving random dot pattern centered over the receptive field of the multiunit activity. We observed considerable heterogeneity in the responses of MT neurons to these search stimuli. Many MT neurons responded well to both stimuli, but we frequently encountered neurons that responded much better to one than to the other. After isolating the signal of a single MT neuron, we mapped its receptive field (minimum response field) using a moving bar whenever possible, and we then placed over the screen a circular aperture whose size and lo-

cation matched the receptive field. We attempted to match the size of the aperture to the size of the receptive field for two reasons: (1) to ensure that the psychophysical observer and the single neuron had equal opportunity to integrate motion signals over space, and (2) to ensure that stimulus-specific effects from regions remote from the receptive field would not affect the single-unit data (Allman et al., 1985a,b). For neurons whose receptive field boundaries could not be precisely established with bars, we adjusted the size and/or location of the aperture to maximize the neuron's response to random dot stimuli. We then determined the neuron's preferred direction and preferred speed using random dot stimuli. If the neuron was tightly tuned for direction, the preferred–null axis could be reliably identified by qualitative judgements of neural responses on an auditory monitor. If the neuron was broadly tuned or inconsistent in its response, identification of the preferred–null axis was made by examining raster displays of neural activity from a computer-controlled direction series. Estimates of preferred speed were always made by listening to neural activity on the audio monitor.

Behavioral paradigms and data collection

After determining the preferred direction and speed for a neuron, we began collection of quantitative data. The data reported in this article were obtained in three types of experiments.

Direction tuning series. The goal of this experiment was to measure quantitatively the direction tuning properties of the neuron. The monkey was rewarded simply for maintaining fixation within an electronically defined window around the fixation point. In most experiments, the window permitted eye movements up to 1.2° from the fixation point, although mean eye position was much closer to the fixation point for the large majority of fixation intervals. While the monkey fixated, 100% correlated random dot patterns near the optimal speed were presented in eight randomly interleaved directions at intervals of 45°. Between 5 and 10 repetitions of each stimulus were obtained, depending upon the reliability of the neuron's responses.

Combined threshold series. This experiment was the primary source of data reported in this article; the experimental goal was to measure neuronal and psychophysical thresholds for discriminating opposite directions of motion. Within a single block of trials, motion signals over a range of correlations were presented in random order both in the neuron's preferred direction and in the null direction. The speed of the motion signal was held constant at the neuron's preferred speed. The range of correlation levels was chosen to span psychophysical threshold and typically included 0% correlation (pure noise) as well. In early experiments the sampled correlation values differed by a factor of the square root of two (1.41), but we soon realized that this provided needlessly fine resolution of the correlation–response function, and subsequently we used values spaced by factors of 2. A block of trials consisted of 15 trials in both the preferred and null directions at each of 6–10 correlation levels.

The structure of an individual trial is illustrated in Figure 2. Figure 2A shows the spatial arrangement of the fixation point, receptive field, stimulus aperture, and target LEDs. Figure 2B illustrates the sequence of events in time. Each trial began with the onset of a fixation point (FP). After the monkey established fixation, a random dot pattern containing a specified motion signal appeared within the stimulus display aperture (Fig. 2B, Stimulus). The monkey viewed the stimulus for 2 sec, during which time it was required to maintain fixation within a criterion distance (typically 1.25°) of the fixation point. Thus, the monkey judged the direction of motion by attending to a stimulus located within the receptive field of the neuron. At the end of the inspection interval, the fixation point and the random dot pattern were extinguished, and two LEDs appeared, corresponding to the two possible directions of stimulus motion, preferred and null (Fig. 2A, Pref LED and Null LED). The monkey reported the direction of the correlated motion signal by making a saccadic eye movement to the corresponding LED. In the example of Figure 2A, the monkey indicated the presence of upward motion during the viewing interval by making a saccade to the "Pref" LED. Similarly, the monkey indicated the presence of downward motion by making a saccade to the "Null" LED. The monkey was required to indicate its decision within 2.1 sec following onset of the target LEDs. Correct decisions were rewarded with a drop of water or juice; incorrect decisions were punished by a brief time-out interval between trials. The monkey was rewarded randomly on half of the trials that contained no motion signal (0% correlation).

Eye movements were measured throughout the experiment using the scleral search coil technique. If the monkey broke fixation at an inap-
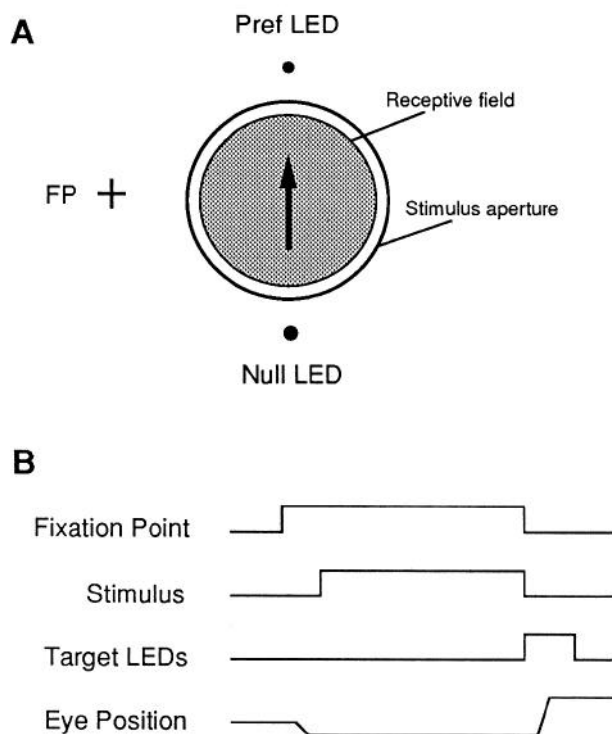
A

Pref LED
•

Receptive field

FP +

Stimulus aperture

•
Null LED

B

Fixation Point

Stimulus

Target LEDs

Eye Position

Figure 2. A schematic description of the psychophysical paradigm employed in this study. *A*, Spatial layout of the fixation point (*FP*), receptive field (*shaded circle*), visual display aperture (*outside circle*), and target LEDs (*Pref* and *Null*). The spatial arrangement of aperture location and preferred–null motion axis was varied across experiments to match the receptive field properties of the neuron under study. *B*, Temporal sequence of events during an individual trial. A trial began with the appearance of a fixation point. After the monkey achieved fixation (*Eye position*), the visual stimulus appeared within the display aperture and remained on for 2 sec. At the end of the display interval, the fixation point and visual stimulus were extinguished and the monkey indicated its judgement of motion direction by making a saccadic eye movement to one of the two target LEDs.

propriate time, the trial was terminated and the data discarded. Similarly, the data were discarded if the monkey failed to make a saccade to one of the two target LEDs within the specified period of time. Failures to make a saccade occurred very rarely since the monkey always had a 50% chance of obtaining a reward simply by guessing.

We successfully completed at least half a block of the combined threshold series (seven trials per condition) on all 216 neurons whose results contribute to our analysis; a full block was completed for 198 of these neurons. If time and isolation permitted, we continued to collect data for up to six repetitions (90 trials per stimulus) of the threshold series.

Physiological threshold series. The goal of this experiment was to determine whether neuronal thresholds were influenced by the monkey's use of the visual stimulus. In this experiment, the monkey was rewarded simply for maintaining fixation during the 2 sec presentation of the visual stimulus; it was *not* required to make a decision concerning the direction of motion in the visual stimulus. The monkey was cued to the type of experiment being conducted within a given block by the color of the fixation point (yellow for the combined threshold series; red for the physiological threshold series) and by the lack of visible saccade targets during the physiological threshold series. The monkey never made saccades to "expected" target locations in the absence of visible targets during the physiological threshold series. Other procedural aspects of the measurements such as stimulus conditions, randomization of stimulus order, and so on, were identical for the two types of blocks.

We obtained data in the physiological threshold series from 86 neurons in two monkeys. For each of the 86 neurons, we gathered only one block of trials using the physiological threshold series, choosing to de-

vote the bulk of experimental time to the combined threshold series. In comparing neuronal thresholds measured under these two conditions (e.g., Fig. 12), we used only a single block of data from the combined threshold series so that the two threshold estimates were based on similar amounts of data. To minimize the effects of long-term fluctuations in neuronal responsiveness, we used the block of data from the combined threshold series that was nearest in time to the block of data obtained in the physiological threshold series. All other thresholds reported in this article are based on the complete set of data obtained for each neuron in the combined threshold series.

Animal training

The animals were trained using operant conditioning techniques with water or juice being the reward for desired behavior. Following surgical preparation, each animal was trained on a sequence of tasks leading up to the two-choice task illustrated in Figure 2. This sequence included (1) fixation, (2) fixation followed by a saccade to a single target, (3) saccade to a single target in the presence of random dot patterns, and (4) choosing between two saccade targets based on the direction of motion in the random dot pattern. Two weeks were generally required for the animal to learn the two-choice task for a single stimulus configuration; strong motion signals (100% correlation) were employed during this initial training period. The monkeys then learned to perform the task at psychophysical threshold. Working the animals down to a stable threshold was a lengthy process, requiring about 4 weeks. After threshold performance was established for the initial set of conditions, the monkey was taught to generalize the task over a number of dimensions including variations in aperture size, aperture location, dot speed, and axis of motion for the direction discrimination. This generalization process was even more lengthy, requiring another 3–5 months of training because threshold performance with one set of conditions did not transfer easily to other sets of conditions. Psychophysical thresholds inevitably rose when the conditions were changed during training, and it was necessary to reestablish asymptotic threshold performance. Condition-specific training effects of this nature (including topographic location and direction of motion) have been reported for human subjects (e.g., Ball and Sekuler, 1982, 1987), but were more pronounced in our monkeys. At the end of the 4–6 month training period, however, the monkeys could generate psychophysical thresholds comparable to human thresholds under a sufficiently wide range of conditions that it was possible to tailor psychophysical discriminanda to the receptive field properties of virtually any MT neuron encountered during our electrophysiological recordings.

In the early stages of training on the two-choice task, the monkeys frequently developed a spatial position habit, making saccadic eye movements predominantly to one of the two saccade targets. To discourage this strategy, we included "correction trials" in all of our two-choice psychophysical paradigms (Mishkin and Weiskrantz, 1958; Cowey and Weiskrantz, 1968; Merigan, 1980; Newsome and Pare, 1988; Pasternak et al., 1989). Correction trials consisted of a series of trials in which motion was presented repeatedly in the neglected direction. Correction trials began if a monkey made incorrect choices on three consecutive presentations of motion in one direction and continued until the monkey chose the neglected direction correctly. Correction trials occurred infrequently after the animals were well trained; data collected on correction trials was not included in the analyses of psychophysical or neuronal performance.

Neuronal data base

The results presented in this article are based on quantitative data obtained from 216 neurons in three monkeys. The responses of 569 neurons were screened during these experiments, but the majority of the neurons were eliminated from the final data base because isolation was not maintained long enough to characterize neuronal and psychophysical responses in the combined threshold series (see above). A minority of the neurons were eliminated, however, because they failed to meet one of two additional inclusion criteria: (1) adequate responsiveness to random dot stimuli, or (2) direction selectivity to random dot stimuli. In practice these criteria were not particularly stringent. We attempted to record from all responsive neurons regardless of the amplitude of the response, but for obvious reasons we quickly abandoned the occasional neuron that was completely unresponsive to random dot stimuli.

The criterion of direction selectivity was imposed because the central goal of these experiments was to compare neuronal and psychophysical
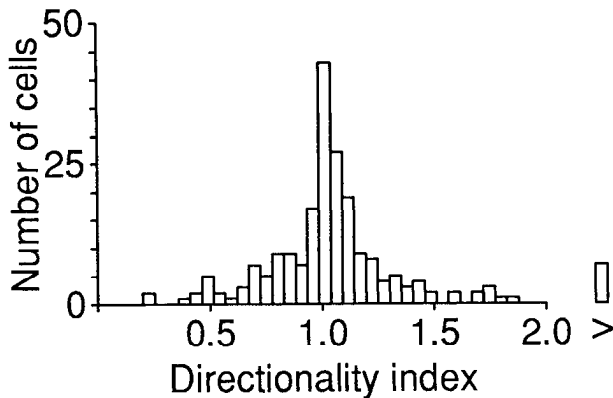
Figure 3. The distribution of direction indices for the 216 neurons studied during these experiments. We used the conventional direction index, $1 - N/P$, where N is the response of the neuron to null direction motion and P is the response to preferred direction motion. Values of the index near zero indicate poor direction selectivity, while values near or greater than unity indicate strong direction selectivity. The distribution is centered about 1.0, indicating a preponderance of highly direction selective neurons.

thresholds for discriminating motion direction. Again, however, this criterion was sufficiently inclusive that very few neurons were eliminated because of it. In practice, a neuron was considered directional if the distribution of response amplitudes evoked by preferred direction motion (100% correlated stimuli) did not overlap with the distribution evoked by null direction motion. This judgement was generally made on line by the experimenter, based either on qualitative evaluation of the audio signal or on visual inspection of raster displays. Note that many directionally biased neurons were admitted by this criterion: both preferred and null direction responses could be excitatory as long as the distributions of their magnitudes did not overlap. We computed a conventional index of directionality for each of the 216 neurons in our data base, and the distribution of indices is shown in Figure 3. This distribution strongly resembles those obtained in several labs from random samples of MT neurons (Baker et al., 1981; Maunsell and Van Essen, 1983b; Albright, 1984); only a handful of neurons at the extreme nondirectional end of the distribution were excluded from our sample.

Table 1 provides a breakdown of the data base on an animal-by-animal basis. The combined sample was distributed reasonably evenly across the three animals. We attempted to record from a similar range of eccentricities in each animal so as to facilitate interanimal comparisons. The geometric mean eccentricity of the receptive field centers was 10.3° in monkey E (range, 5.4–17.1°), 6.8° in monkey J (range, 1.4–16.4°), and 7.6° in monkey W (range, 1.3–31.4°). Despite the general similarity of these ranges, a one-way ANOVA revealed significant differences in receptive field eccentricity among the three animals ($p <$ 0.0001). Eccentricities were indistinguishable between monkey J and monkey W (test of contrasts, $p >$ 0.05), but were significantly greater in monkey E ($p <$ 0.05).

Since we always tailored the psychophysical discrimination task to match the properties of the neuron under study, considerable variability occurred from experiment to experiment in the size of the stimulus aperture and in the speed of the correlated motion signal. Within the sample of 216 neurons, aperture sizes ranged from 2.5° to 20° in diameter, and preferred speeds ranged from 0.4 degrees/sec to 28.4 degrees/sec. Both receptive field size and preferred speed were positively correlated with eccentricity.

Histology

During recording experiments MT was identified on the basis of reliable physiological criteria as described above. One of the three monkeys employed in the present study is still alive and being used in related experiments, but histological analysis has been performed on the brains of the other two animals. The two animals were killed by an overdose of barbiturate (sodium pentothol) and perfused transcardially with normal saline followed by 10% formalin fixative. The brains were removed, blocked, and equilibrated in 30% sucrose. Frozen sections were cut in the sagittal plane at 48 μm thickness. Alternate series (at 500 μm in-

Table 1. Breakdown of neuronal data base for the experiments reported in this article

Monkey	Guide tubes	Penetrations	Cells screened	Cells included
E	6	42	94	52
J	22	142	258	77
W	20	153	217	87

tervals) were stained for cell bodies with cresyl violet and for myelinated fibers using a modification of the Gallyas (1979) reduced silver method. While the tracks of most penetrations made over a period of several months were impossible to reconstruct, the region from which we recorded was evident from scars left by the guide tubes and from occasional electrode tracks observed within the posterior bank of the superior temporal sulcus. In both monkeys, the region thus identified corresponded well to the location of MT as identified in the myelin-stained sections (Allman and Kaas, 1971; Ungerleider and Mishkin, 1979; Van Essen et al., 1981).

Results

Analysis of psychophysical data. Figure 4 illustrates typical psychophysical data obtained during a combined threshold series. The data are displayed as a psychometric function in which the proportion of correct decisions is plotted against the correlation level of the motion signal. In general, the correlation levels were chosen so that the monkey performed perfectly for the strongest motion signals but performed at chance (50% correct) for the weakest signals. We used a maximum-likelihood method (Watson, 1979) to fit these data with functions of the form

$$p = 1 - 0.5 \exp[-(c/\alpha)^\beta], \qquad (1)$$

where p is the probability of a correct decision, c is the correlation of the motion signal, α is the correlation level supporting "threshold" performance (82% correct), and β is the slope of the function. This function is derived from the integral of the Weibull distribution, and was first applied to psychophysical data in this manner by Quick (1974). Figure 4 illustrates such a curve fitted to the psychophysical data obtained in one of our
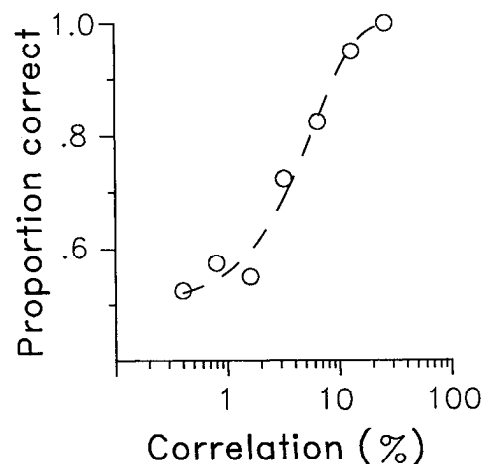

Figure 4. A typical psychometric function obtained during study of a single MT neuron. The *abscissa* shows the strength of the motion signal, and the *ordinate* indicates the monkey's performance. Each psychometric function was fit with sigmoidal functions of the form given in Equations 1 and 2. For this experiment, psychophysical threshold (α) was 6.1% correlation; the unitless slope parameter (β) for the psychometric function was 1.17.

experiments. The threshold parameter, α (6.1% correlation), and the slope parameter, β (1.17), provide a convenient reduction of the psychophysical data, and we will use them extensively in subsequent descriptions of our results.

The function in Equation 1 generally fitted our data well; the fit could be rejected for only 32 of the 216 psychometric functions in our data set (χ^2, $p < 0.05$). Visual inspection of the problematic functions revealed that failure of the fit often resulted from a small number of errors at the highest correlation level. In such instances, the Weibull fit could be improved with a modification of Equation 1 that permitted the asymptotic performance level to be a free parameter in the maximum-likelihood fitting routine. In this formulation, Equation 1 becomes

$$p = \delta - (\delta - 0.5) \exp[-(c/\alpha)^\beta], \qquad (2)$$

where δ is the asymptotic performance level at high correlation levels expressed as proportion correct. Fits to the psychometric data provided by Equation 2 could be rejected for only 16 of the 216 experiments (7.4%). In general, then, Equations 1 and 2 provided a good description of our psychophysical data.

Most values of α and β reported in this article were taken from the best-fitting solution to Equation 1. In a minority of cases (38 of 216 psychometric functions), values were taken from Equation 2 because it provided a significantly better fit to the data.

Analysis of physiological data. Figure 5 illustrates physiological data obtained during the same combined threshold series as the psychophysical data in Figure 4. We recorded from this neuron long enough to obtain 60 trials in both the preferred and null directions for seven different correlation levels. We considered the neuron's response on each trial to be the total number of action potentials that occurred during the 2 sec viewing interval. The frequency histograms in Figure 5A show the distribution of responses obtained from this neuron at five correlation levels. The open bars indicate responses to motion in the preferred direction; the solid bars indicate responses to motion in the null direction. At 12.8% correlation, the neuron was highly direction selective: the responses elicited by preferred direction motion were larger than all but a few responses elicited by null direction motion. As the correlation level was reduced, however, the neuron became progressively less directional. At 0.8% correlation, the response distributions for preferred and null direction motion were virtually identical. Over this range of correlation levels, then, the neuron crossed a threshold for encoding directional information that is qualitatively similar to the direction discrimination threshold in the psychophysical data of Figure 4.

In analyzing these physiological data, our goal was to produce a quantitative description of neuronal sensitivity that was directly comparable to the description of psychophysical sensitivity captured in the psychometric function. We therefore employed a method based on signal detection theory (Green and Swets, 1966) to compute a "neurometric function" for each cell (Barlow et al., 1971; Cohn et al., 1971; Tolhurst et al., 1983; Bradley et al., 1987; Vogels and Orban, 1990). These functions reflect the probability that an ideal observer could accurately report the direction of correlated motion in the visual stimulus, basing his judgements on responses like those recorded from the neuron under study. This probability increases from chance at low correlation levels to unity at high correlation levels, and the resulting neurometric function can be quantitatively com-

pared to the actual psychometric function obtained from the monkey on the same set of trials. This signal detection based method of analysis has the additional advantage that it requires no assumptions concerning the shape of the neuronal response distributions illustrated in Figure 5A.

To compute the neurometric function, we made the simplifying assumption that neuronal thresholds could be meaningfully computed by comparison of two signals, corresponding to those from the neuron under study and those from a hypothetical "antineuron," identical in all respects save that its preferred direction was in the opposite direction. We then suppose that on any given trial, the decision is made in favor of the direction preferred by the neuron yielding the larger response. (We assume that the responses of the neuron and antineuron are statistically independent, although performance could in principle be computed with varying amounts of correlation between neuron and antineuron.) It is important to note that we use this two-neuron decision model simply as a tool for analyzing the directional sensitivity of single MT neurons. We explored an alternative method for computing single-cell thresholds that did not involve an explicit neuron–antineuron comparison (e.g., Tolhurst et al., 1983), but the alternative approach did not lead to qualitatively different conclusions from those presented here. We will take up in the Discussion the question of what kind of model can best be used to understand the actual psychophysical decision process.

Under these simple assumptions, the frequency histograms in Figure 5A can be considered to represent the responses of both the neuron and the antineuron to a single direction of motion: the measured responses of the *neuron* to *null* direction motion are transposed to represent the responses of the *antineuron* to *preferred* (for the *neuron*) direction motion. On a single trial, therefore, the decision will result from a comparison of a response drawn randomly from an open-bar distribution in Figure 5A with a response drawn randomly from the solid-bar distribution at the same correlation level. The decision will be "correct" if the draw from the open-bar distribution is larger than the draw from the solid-bar distribution. Conversely, the decision will be "incorrect" if the draw from the solid-bar distribution is larger. From the data in Figure 5A, one can see intuitively that the decisions produced by this analysis will be correct on a very large percentage of the trials at 12.8% correlation, because there is very little overlap in the two distributions. Performance will be near chance (50% correct) for 0.8% correlation, because the two distributions overlap completely.

To compute performance, we compiled an ROC (receiver operating characteristic; Green and Swets, 1966) for each pair of preferred and null direction response distributions. Figure 5B illustrates the family of ROCs for the five correlation levels whose response distributions are shown in Figure 5A. Each ROC is generated by plotting, for all possible criterion response levels, the proportion of preferred direction trials on which the response exceeded criterion against the proportion of null direction trials on which the response exceeded criterion (Tolhurst et al., 1983). At 12.8% correlation, for example, all trials in *both* the preferred and null direction distributions exceeded a criterion response level of 1 impulse/trial, and the resulting point on the ROC fell in the upper right corner of the unit square in Figure 5B. As the criterion increased to 50 impulses/trial, the proportion of null direction responses exceeding criterion fell nearly to zero while the proportion of preferred direction responses exceeding criterion remained near unity. As the criterion increased further
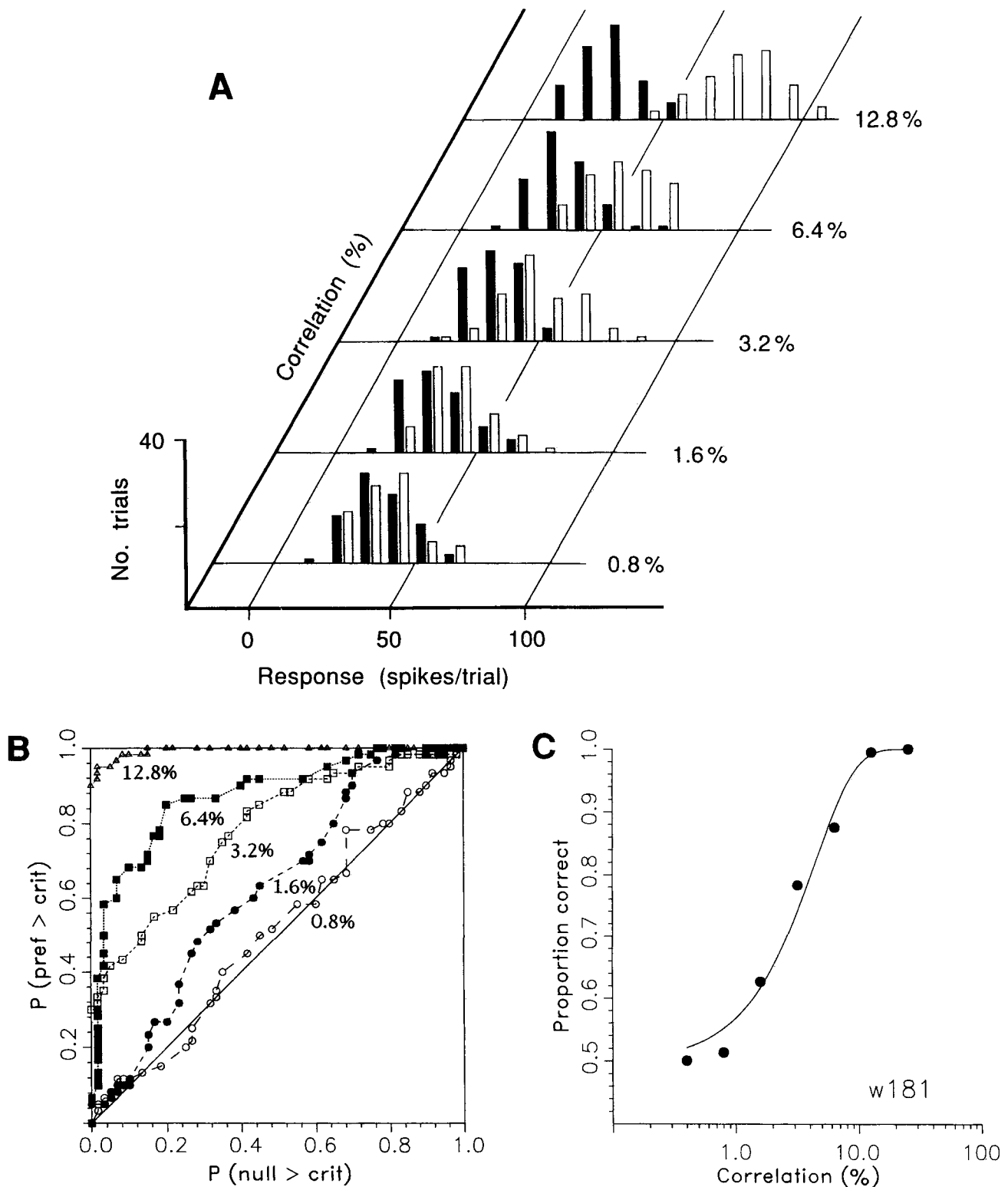
Figure 5. Analysis of physiological data. *A*, This three-dimensional plot illustrates frequency histograms of responses obtained from a single MT neuron at five different correlation levels. The *horizontal axis* shows the amplitude of the neuronal response, and the *vertical axis* indicates the number of trials on which a particular response was obtained. The *depth axis* shows the correlation of motion signal used to elicit the response distributions. *Open bars* depict responses obtained for motion in the neuron's preferred direction, while *solid bars* illustrate responses for null direction motion. For this neuron, each distribution is based on 60 trials. *B*, ROCs for the five pairs of preferred–null response distributions illustrated in *A*. Each point on an ROC depicts the proportion of trials on which the preferred direction response exceeded a criterion level plotted against the proportion of trials on which the null direction response exceeded criterion. Each ROC was generated by increasing the criterion level from 0 to 120 spikes in one-spike increments. Increased separation of the preferred and null response distributions in *A* leads to an increased deflection of the ROC away from the diagonal. *C*, A neurometric function that describes the sensitivity of an MT neuron to motion signals of increasing strength. The *curve* shows the performance of a simple decision model that bases judgements of motion direction on responses like those illustrated in *A*. The proportion of correct choices made by the model is plotted against the strength of the motion signal. The proportion of correct choices at a particular correlation level is simply the normalized area under the corresponding ROC curve in *B*. For this neuron, data were obtained at seven correlation levels; response distributions and ROC curves are illustrated for five of these levels in *A* and *B*. The neurometric function was fitted with sigmoidal curves of the form given in Equation 1. In this experiment, neuronal threshold (α) was 4.4% correlation and the unitless slope parameter for the neurometric function (β) was 1.30.
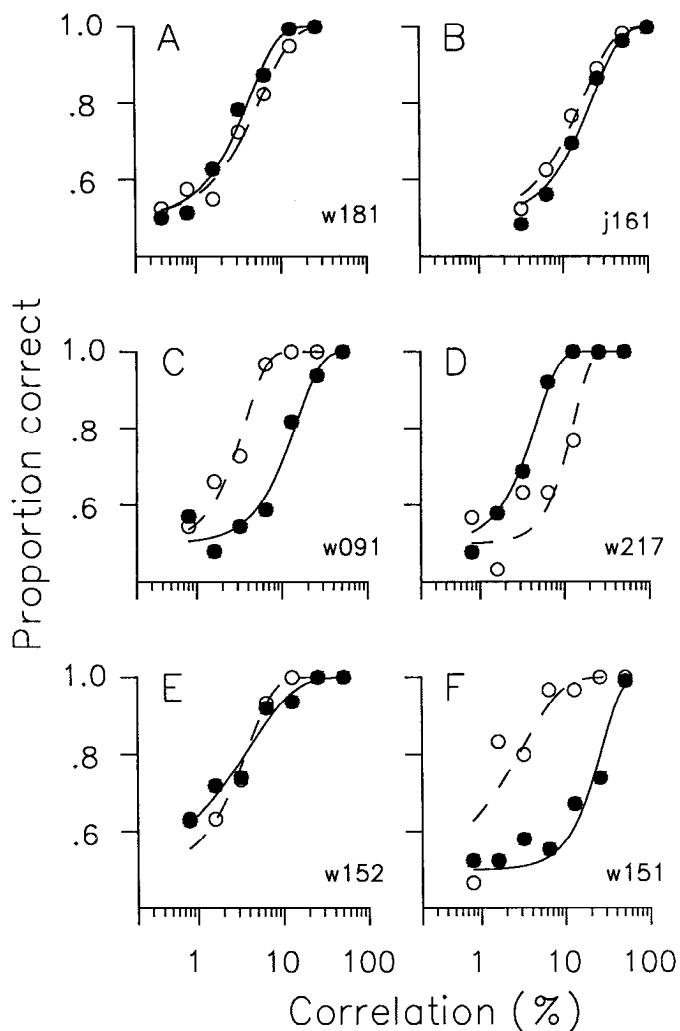
Figure 6. Psychometric and neurometric functions obtained in six experiments. The *open symbols* and *broken lines* depict psychometric data, while the *solid symbols* and *solid lines* represent neurometric data. The six examples illustrate the range of relationships present in our data. *A,* Results of the experiment illustrated in Figures 4 and 5. Psychophysical and neuronal data were statistically indistinguishable in this experiment. Thresholds and slope parameters are given in the captions for Figures 4 and 5. *B,* A second experiment in which psychometric and neurometric data were statistically indistinguishable. Psychometric α = 17.8% correlation, β = 1.20; neurometric α = 23.0% correlation, β = 1.31. *C,* An experiment in which psychophysical threshold was substantially lower than neuronal threshold. Psychometric α = 3.7% correlation, β = 1.68; neurometric α = 14.8% correlation, β = 1.49. *D,* An experiment in which neuronal threshold was substantially lower than psychophysical threshold. Psychometric α = 13.0% correlation, β = 2.15; neurometric α = 4.7% correlation, β = 1.58. *E,* An experiment in which thresholds were similar but slopes were dissimilar. Psychometric α = 3.9% correlation, β = 1.36; neurometric α = 4.0% correlation, β = 0.79. *F,* An experiment in which threshold and slope were dissimilar. Psychometric α = 3.1% correlation, β = 0.91; neurometric α = 27.0% correlation, β = 1.81.

to 120 impulses/trial, the proportion of preferred direction responses exceeding criterion also fell toward zero. Thus, the ROC for 12.8% correlation fell along the upper and left margins of the unit square in Figure 5B (triangles). In contrast, the ROC for 0.8% correlation fell near the diagonal line bisecting the unit square (open circles); since the preferred and null response distributions were very similar at 0.8% correlation, the proportion of preferred and null direction responses exceeding criterion fell

at roughly equal rates as the criterion response increased from 1 to 100 impulses/trial. In general, the curvature of the ROC away from the diagonal indicates the separation of the preferred and null response distributions (Bamber, 1975).

Green and Swets (1966) showed formally that the normalized area under the ROC corresponds to the performance expected of an ideal observer in a two-alternative, forced-choice psychophysical paradigm like the one employed in the present study. Again, one can intuit that this is reasonable. At 12.8% correlation, 99% of the area of the unit square in Figure 5B falls beneath the ROC, corresponding to the near-perfect performance we would expect based on the response distributions for 12.8% correlation in Figure 5A. In contrast, only 51% of the unit square falls beneath the ROC for 0.8% correlation, corresponding as expected to random performance.

For each correlation level tested, we used this method to compute the probability that the decision rule would yield a correct response, and the results are shown in Figure 5C. These data capture the sensitivity of the neuron to directional signals in the same manner that the psychometric function captures perceptual sensitivity to directional signals. As for the psychometric data, we fitted the neurometric data with smooth curves of the form given by Equation 1. This function provided an excellent description of the neurometric data; the fit could be rejected for only 2 of the 216 neurometric functions in our data set (χ^2 test, $p < 0.05$). Application of Equation 2 resulted in a significantly improved fit for only one neuron. For the example in Figure 5C, the threshold parameter, α, was 4.4% correlation, and the slope parameter, β, was 1.30. For each neurometric function, these parameters can be compared to the equivalent parameters obtained from the corresponding psychometric function.

Comparison of psychometric and neurometric functions. Figure 6A shows the psychometric and neurometric functions obtained from the experiment illustrated in Figures 4 and 5. The two functions are remarkably similar both in their location along the abscissa and in their overall shape. The apparent similarity of the two functions was reflected in a close correspondence between the threshold parameters, α, and the slope parameters, β, obtained from the Weibull fits (Eq. 1) to the two data sets. The neurometric threshold of 4.4% correlation compared favorably to the psychometric threshold of 6.1% correlation, and the slope parameters were similar as well (neurometric β = 1.30; psychometric β = 1.17). This similarity of psychometric and neurometric data was a common feature of our data, and Figure 6B illustrates a second example. Although the absolute threshold levels were higher under the conditions of this experiment, the neurometric and psychometric data sets were again quite similar (neuronal: α = 23.0%, β = 1.31; psychophysical: α = 17.8%, β = 1.20). Higher absolute thresholds typically occurred when the properties of the neuron under study required a psychophysically nonoptimal presentation of the discriminanda (e.g., unusually small receptive fields, large eccentricities, or high speeds). The remaining panels in Figure 6 exemplify the range of variation in our data. Neuronal and psychophysical thresholds could be strikingly dissimilar, with either the neuron (Fig. 6D) or the monkey (Fig. 6C,F) being more sensitive. The slope parameters could also appear dissimilar (Fig. 6E,F), but significant differences in slope were observed less frequently than significant differences in threshold (see below).

A particularly surprising aspect of our data was the existence of MT neurons that were substantially more sensitive to motion

signals in the visual display than was the monkey psychophysically. In the experiment of Figure 6D, for example, the neuronal threshold (4.7% correlation) was considerably lower than the psychophysical threshold (13.0% correlation). This result could obtain trivially if the monkey's performance were deteriorating near the end of a recording session due to water satiation, or if the monkey's performance were suboptimal due to a lack of training under the specific psychophysical conditions of the experiment. The first explanation is ruled out by the fact that our monkeys' performance in these experiments was highly reliable, as indicated both by their asymptotic performance levels at high correlation levels (near 100% correct) and by the steepness of their psychometric functions (see Fig. 6D). Indolence is generally reflected by deterioration in both of these features of the psychometric data. The second explanation seems unlikely since our monkeys' psychophysical thresholds were usually similar to the thresholds of human observers across the range of conditions tested in these experiments. We therefore believe that neurons such as the one illustrated in Figure 6D are genuinely more sensitive to the motion signals than is the visual system overall as reflected in psychophysical performance. Another way of thinking about this result is that the monkey could improve its performance considerably were it able to monitor signals from a neuron like the one in Figure 6D (and its antineuron partner) and count action potentials with the accuracy of our computer.

For each experiment, we assessed the similarity of the neurometric and psychometric functions with a statistical test for the homogeneity of the two data sets. We performed maximum likelihood fits of separate Weibull functions to the neurometric and psychometric data, and also fit the best single function jointly to the two data sets. The likelihoods (L) obtained from these two conditions were transformed by

$$\lambda = -2 \ln\left(\frac{L(\text{data} \mid \text{single curve})}{L(\text{data} \mid \text{independent curves})}\right), \qquad (3)$$

so that λ is distributed as χ^2 with 2 degrees of freedom (see Hoel et al., 1971). If λ does not exceed the criterion value (for $p = 0.05$), we conclude that a single function fits the two data sets no worse than two separate functions.

For 109 of 216 cells (51%), this method revealed no significant difference between Weibull fits to psychometric and neurometric data. This result might arise artifactually if the data from either the neuron or psychophysics were not well fit by the Weibull function. However, for only 11 of these 109 cells could the fit to either behavioral or neural data be rejected. We also compared the psychophysical data to neurometric predictions of performance using a different method that did not rely on fitting the data to a particular function; we normalized the binomially distributed decision values using the arcsin-square-root transformation (Johnson and Kotz, 1969), and computed a conventional χ^2 test of homogeneity. We compared the number of correct decisions observed behaviorally to the number predicted from single-unit recording, where

$$\text{Predicted correct} = (N/2)\ (\text{Area under ROC}). \qquad (4)$$

The estimate uses half the number of trials $(N/2)$ because the ROC computation assumes two independent measures of unit response (e.g., neuron and antineuron as described above). This statistic identified only two additional neurons for which neurometric predictions differed significantly from psychophysical performance. We therefore conclude that neurometric and psy-
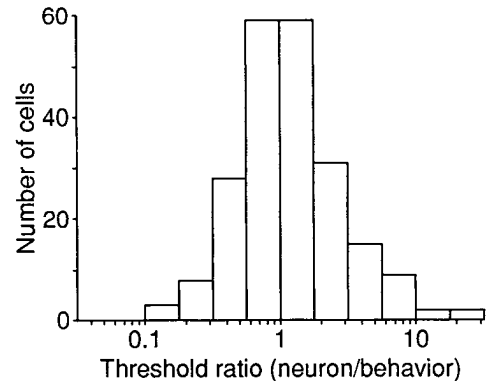

Figure 7. Relative sensitivity of single MT neurons and animal observers. The frequency histogram illustrates the ratio of neuronal threshold to psychophysical threshold for the 216 experiments in our sample. Ratios less than unity indicate that the neuron was more sensitive than the monkey; ratios above unity indicate the converse.

chometric data were genuinely indistinguishable in roughly half (109 of 216) of our experiments.

For the remaining 107 cells (49%), we found a significant difference between the Weibull fits to the psychometric and neurometric data. For these cells, we wished to know whether the discrepancy was due to a difference in the threshold or the slope of the functions characterizing the two data sets. We again compared Weibull fits to the neural and behavioral data under the null hypothesis that the data are described by a single curve, versus the alternative of separate fits for neural and behavioral data, but we further elaborated the test so that three conditions were compared: (1) assuming a common threshold parameter (α) in the two fits, (2) assuming a common slope parameter (β), or (3) allowing slope and threshold to vary freely in the two fits. If a significant difference between neurometric and psychometric fits was obtained when the slope was constrained, we attributed the difference to the thresholds. Similarly, a significant difference obtained when the threshold was constrained indicated that the disparity lay in the slopes. Employing this approach, we found that most of the discrepancies (78 of 107 cells) were due to differences in the threshold (e.g., Fig. 6C,D,F). In only 10 neurons could the difference be ascribed to the slope; for the remaining 19 neurons, the discrepancy between neuron and behavior was not due to differences in either the slope or the threshold alone.

The similarity of neurometric and psychometric functions is represented graphically in Figures 7 and 8. Figure 7 is a frequency histogram of threshold ratios that summarizes the comparison of neuronal and psychophysical thresholds for all 216 experiments. Ratios near unity resulted from experiments such as those in Figure 6, *A, B,* and *E,* where neuronal and psychophysical thresholds were very similar. Ratios below unity signify experiments like that in Figure 6D, in which the neuron was more sensitive than was the monkey psychophysically; ratios above unity represent experiments in which psychophysical judgement was more sensitive (e.g., Fig. 6C,F). The data in Figure 7 are distributed roughly normally on the logarithmic scale, and include a wide range of threshold ratios. The most striking feature of the distribution, however, is that the ratios were centered very near unity: the geometric mean of the distribution was 1.19. Across the entire set of data, therefore, average neuronal sensitivity was surprisingly similar to average psychophysical sensitivity.
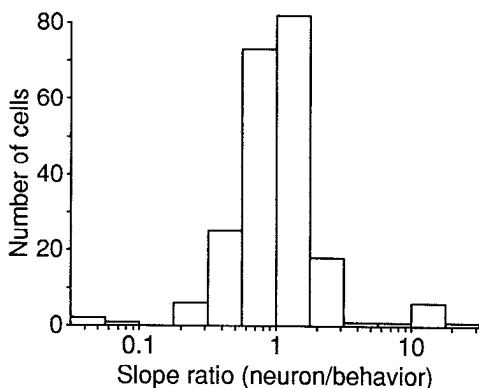
Figure 8. Relative slopes of neurometric and psychometric functions. The frequency histogram illustrates the ratio of neurometric slope to psychometric slope for the 216 experiments in our sample. Ratios less than unity indicate that the psychometric slope was steeper than the neurometric slope; ratios above unity indicate the converse.

We next conducted a one-way ANOVA to determine whether the distribution of threshold ratio differed among the three animals. The analysis indeed revealed a significant difference ($p < 0.0005$), and the difference withstood an analysis of covariance that controlled for the effects of several potentially confounding independent variables: aperture eccentricity, aperture size, and motion speed ($p < 0.0001$). A test of contrasts showed that the threshold ratios for monkey J differed significantly from those of both monkey W and monkey E ($p < 0.0001$), but the threshold ratios of the latter two animals were not significantly different from each other ($p > 0.05$). The interanimal differences, though significant, were small: the geometric mean of the threshold ratio was 0.89 in monkey J, 1.21 in monkey E, and 1.51 in monkey W. We conclude, therefore, that a close correspondence of neuronal threshold to psychophysical threshold was a characteristic feature of MT neurons for all three monkeys under the conditions of our experiment.

Figure 8 shows the distribution of slope ratios obtained from the 216 experiments in our sample. Like the threshold ratios, the slope ratios were logarithmically distributed with a geometric mean very near unity (0.995). There is less scatter in this distribution than in the distribution of threshold ratios in Figure 7, consistent with the statistical analysis presented above that showed that the hypothesis of common thresholds could be rejected far more frequently than the hypothesis of common slopes. A one-way ANOVA revealed no significant difference among animals ($p = 0.70$). Thus, the similarity in shape of the neurometric and psychometric functions, as illustrated in Figure 6A–D, was typical of our results as a whole.

How well does neuronal threshold predict psychophysical threshold? The data in Figure 7 show that for the majority of neurons in our sample, psychophysical and derived neuronal thresholds are similar. Thus, knowledge of neuronal threshold is frequently an accurate predictor of psychophysical threshold. However, the histogram in Figure 7 intentionally obscures other aspects of the data such as absolute threshold levels and the extent to which departures of threshold from the mean are correlated for neuronal and psychophysical data. We therefore asked two more refined questions: (1) do there exist interanimal differences in psychophysical sensitivity that are predicted by neuronal sensitivity, and (2) does there exist a correlation between neuronal sensitivity and psychophysical sensitivity on an ex-

periment-by-experiment basis? The answer to both of these questions is "yes," although the latter effect is quite modest.

During the course of these experiments, it was our subjective impression that the three monkeys differed in their psychophysical sensitivities to the stochastic motion signals in our visual stimuli. This impression was confirmed by a one-way ANOVA of the 216 psychophysical thresholds in our data set ($p < 0.0001$). The interanimal threshold difference also withstood an analysis of covariance that controlled for the effects of other independent variables that may have varied between monkeys: aperture eccentricity, aperture size, and the speed of the motion signal ($p < 0.0001$). Interestingly, neuronal thresholds in the 216 experiments of our study also differed between animals (analysis of covariance, $p < 0.02$), and the ordinal relationship of mean neuronal threshold for the three animals was the same as that for mean psychophysical threshold.

This relationship is summarized in Figure 9A, which illustrates mean psychophysical threshold as a function of mean neuronal threshold for the three animals. The broken line in Figure 9A is the regression of mean psychophysical threshold onto mean neuronal threshold. This is a maximum likelihood fit based on the geometric mean values of psychophysical α and neuronal α along with their measured uncertainties and covariance, assuming a bivariate lognormal distribution. The slope of this three-point regression is 2.08: This value differs significantly from unity by a likelihood ratio test (as in Eq. 3) in which the fit was compared to a second maximum likelihood regression with slope constrained to unity ($p < 0.0001$). We were somewhat surprised that the slope of the regression line differed from unity, although this finding is consistent with our observation in the preceding section that small but significant differences exist among the three animals in the mean ratio of neuronal to psychophysical threshold. The consistent ordinal relationship between mean neuronal and psychophysical threshold for the three animals supports the notion that psychophysical performance on our task is limited by signals like those carried by MT neurons.

Figure 9B shows the relationship between the geometric means of neuronal and psychophysical slope parameters for the three monkeys. Again, the ordinal relationship in the slope parameter, β, was the same for the two data sets, even though the interanimal differences in neuronal β and psychophysical β missed statistical significance (analysis of covariance, $p = 0.058$ for neuronal β, $p = 0.120$ for psychophysical β). A regression line was fit to the three points using the same method as for Figure 9A. The regression line had a slope of 0.59, but this slope was not significantly different from unity by the maximum likelihood test employed above ($p > 0.05$). Again, the data are consistent with the notion that interanimal differences in psychophysical performance result from interanimal differences in physiological properties like those we observed in MT neurons.

We next inquired whether any correlation exists between neuronal threshold and psychophysical threshold on an cell-by-cell basis. Since several independent variables that influence psychophysical threshold differed among the three animals, we addressed this question by means of a hierarchically structured analysis of covariance. In the first covariance model, the 216 psychophysical thresholds were analyzed as a function of monkey identity, aperture size, aperture eccentricity, and speed of the correlated motion signal. The analysis revealed that each of these independent variables had a significant effect on psychophysical threshold, and the whole model captured about 44%
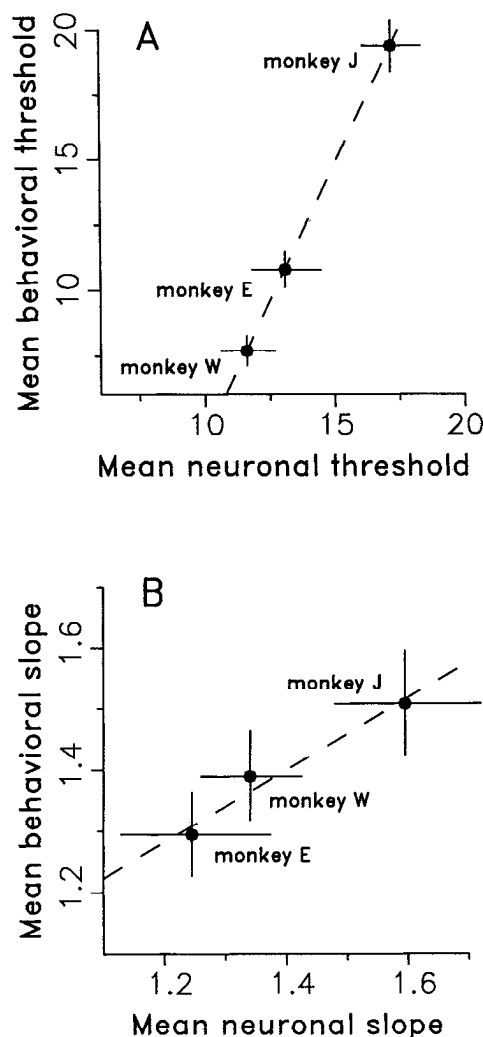
Figure 9. A comparison of average neuronal and psychophysical performance across animals. *A,* The geometric mean of neuronal threshold is plotted against the geometric mean of psychophysical threshold for each of the three animals in the study. The *vertical error bars* indicate SEM for neuronal threshold, while the *horizontal error bars* show SEM for psychophysical threshold. The *broken line* is the best-fitting regression through the data points. *B,* The geometric mean of neurometric slope is plotted against the geometric mean of psychometric slope. Error bars and the regression line are as described in *A.*

Figure 10. A comparison of absolute neuronal and psychophysical threshold for the 216 experiments in our sample. *Solid circles* indicate experiments in which neuronal and psychophysical threshold were statistically indistinguishable; *open circles* illustrate experiments in which the two measures were significantly different. The *broken diagonal* is the line on which all points would fall if neuronal threshold predicted psychophysical threshold perfectly. The frequency histogram at the *upper right* was formed by summing across the scatterplot within diagonally oriented bins. The resulting histogram is a scaled replica of the distribution of threshold ratios depicted in Figure 7.

of the variance in psychophysical α (r^2, the amount of variance accounted for, $= 0.438$). Adding neuronal threshold to the model as a coregressor revealed a significant predictive effect of neuronal threshold ($p < 0.01$), but the effect was small, accounting for only an additional 2% of the variance in psychophysical threshold ($r^2 = 0.458$). Thus, experiment-to-experiment variations in neuronal threshold were not highly correlated with variations in psychophysical threshold, even though the *means* were strikingly similar (e.g., Fig. 7).

Figure 10 amplifies this point by showing the relationship of neuronal to psychophysical threshold in richer detail. The scatterplot depicts the actual neuronal and psychophysical thresholds measured in each of the 216 experiments in our sample. The solid circles indicate experiments in which the neurometric and psychometric functions were statistically indistinguishable as described earlier; the open circles show experiments in which the two data sets were demonstrably different. The broken di-
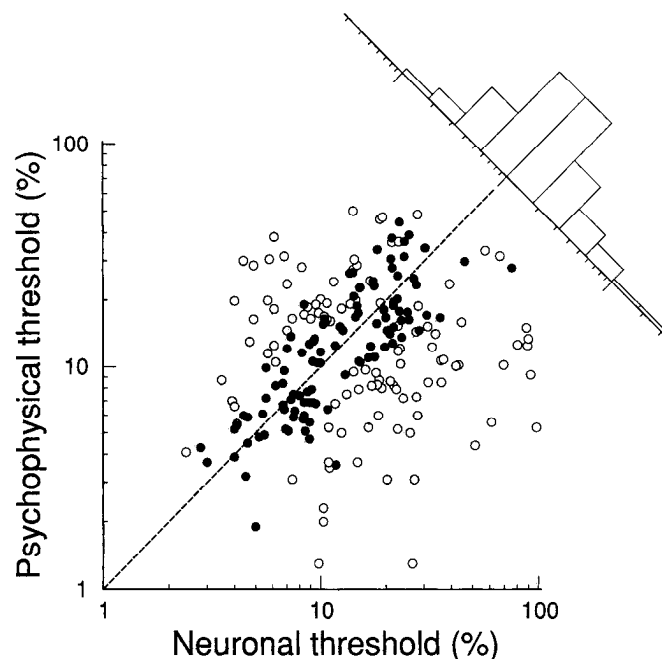
agonal line depicts the line of equality on which all points would fall if neuronal threshold perfectly predicted psychophysical threshold. Summing within a diagonally arranged set of bins leads to the frequency histogram in the upper right corner of Figure 10; this is simply a scaled replica of the distribution of threshold ratios shown in Figure 7. Despite the symmetrical distribution of the ratios about unity, the scatterplot reveals only a modest correlation between the two measures ($r = 0.29$), and most of this correlation is accounted for by the interanimal differences illustrated in Figure 9*A*. Thus, psychophysical and neuronal thresholds are not strongly correlated on an cell-by-cell basis, although they are closely related *on the average.* The absence of a strong cell-to-cell correlation is not surprising since neuronal sensitivity to motion direction varies widely (even within MT) whereas a monkey's psychophysical sensitivity is relatively constant for any given set of stimulus conditions.

Effect of integration time on neuronal and psychophysical thresholds. The comparison of neuronal and psychophysical thresholds summarized in Figure 7 is based on experiments in which the monkey was required to view the random dot stimulus for 2 full seconds before indicating its judgement of motion direction. A potential flaw in the analysis results from the unknown time interval over which the monkey integrated information in reaching its decision. Temporal integration can influence both neuronal and psychophysical thresholds, and the comparison captured in Figure 7 is reasonable only if the integration interval is similar for both sets of data. For the physiological data presented thus far, the integration interval was always 2 sec since construction of the ROCs was always based
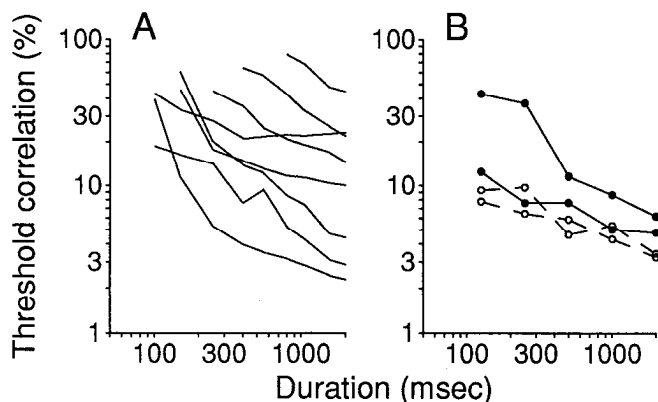
Figure 11. An analysis of integration times for neuronal and psychophysical data. *A*, Threshold as a function of integration time for eight representative MT neurons. Integration times on the abscissa are measured from the onset of the visual stimulus. For each neuron, all data points were based on an analysis of a single experiment in which the visual stimulus remained on for 2 sec. *B*, Psychophysical threshold as a function of integration time for two human (*open symbols*) and two monkey (*solid symbols*) observers. Each data point represents the mean of at least 10 threshold measurements. Thresholds were measured using a staircase procedure (Newsome and Pare, 1988). Unlike the neuronal data illustrated in *A*, psychophysical thresholds for each integration time were measured independently in separate blocks of experiments. All thresholds were measured using a 10° diameter aperture centered on the horizontal meridian 7° to the left of the fixation point. The axis of motion was up versus down, and the speed of the motion signal was 3.6 degrees/sec.

on the cumulative number of spikes occurring during the entire viewing interval. It would be problematic for the analysis in Figure 7, however, if the monkeys reached psychophysical decisions by attending to the visual display for only a small fraction of the 2 sec viewing interval. We therefore assessed the effect of integration time on both physiological and psychophysical results.

To examine the effects of integration time on neuronal threshold, we repeated the ROC analysis several times for each neuron, counting the number of spikes that occurred during progressively longer temporal intervals ranging from 100 msec following stimulus onset to the full 2 sec. This procedure generated a family of neurometric functions for each neuron, from which neuronal thresholds (α) were computed using best-fitting solutions to Equation 1. Figure 11*A* illustrates the results of this analysis for eight example neurons. These eight neurons illustrate the full range of neuronal sensitivities in our sample, from very low-threshold neurons (e.g., the lowest curve in Fig. 11*A*; α = 2.3% correlation at 2 sec) to very high-threshold neurons (e.g., the highest curve in Fig. 11*A*; α = 45.6% correlation at 2 sec). The results were very consistent: neuronal thresholds decreased for progressively longer integration times. This result is expected as a simple consequence of the fact that noise resulting from irregularity in a neuron's firing pattern becomes less pronounced with longer measurement times. As noise is reduced, estimates of the mean firing rate across trials become more consistent (i.e., response distributions like those illustrated in Fig. 5*A* become less variable), and neuronal thresholds consequently fall.

Figure 11*B* illustrates the effect of integration time on psychophysical threshold. These experiments were performed as controls following completion of the physiological recording experiments. The subjects were two humans (open symbols) and

two monkeys (solid symbols) that were used in the physiological experiments (monkey E and monkey J). The third monkey had been killed by the time these psychophysical measurements were made. Each data point in the figure represents the mean of at least 10 threshold measurements for that condition. All thresholds in Figure 11*B* were obtained using blocked stimulus presentations, with integration time held constant during each block. One of the monkeys (monkey E) generated thresholds that were essentially the same as those of the two human subjects, while the other monkey (monkey J) yielded higher thresholds, particularly for short viewing intervals. Both monkey and human subjects practiced extensively at each integration interval to ensure that the psychophysical thresholds in Figure 11*B* represented asymptotic performance. The data were obtained under psychophysical conditions that were similar to the best conditions encountered during the physiological experiments reported in this study (see Fig. 11 caption). Thus, psychophysical thresholds for the 2 sec viewing interval (3–6% correlation) were comparable to the best psychophysical thresholds obtained during the physiological recording experiments illustrated in Figure 10.

The most important result in Figure 11*B* is that psychophysical performance improved with increased viewing time for all four subjects. As noted above, thresholds illustrated for the longest viewing time (2 sec) in Figure 11*B* were typical of those observed for the same viewing time during the prior physiological recording experiments. In other words, training for short viewing times did not seem to change performance for long viewing times. The data indicate that the monkeys, like human subjects, improved their performance by availing themselves of the long integration time offered by the 2 sec viewing interval (Downing and Movshon, 1989). We therefore conclude that our use of the total spike count during the full 2 sec viewing interval provides a legitimate basis for comparing neuronal and psychophysical thresholds.

Influence of behavior on neuronal thresholds. For 86 neurons in two monkeys, we measured neuronal thresholds in the physiological threshold series as well as in the combined threshold series. In the physiological threshold series, the monkey was rewarded simply for maintaining fixation on the fixation point; the random dot stimulus in the receptive field was therefore irrelevant to the animal's behavior. In the *combined threshold series*, the monkey was required to attend to the random dot stimulus (while maintaining fixation) and report the direction of correlated motion in order to obtain a reward. As described in Materials and Methods, the monkey could easily distinguish the two blocks of trials by the color of the fixation point and by the absence of saccade targets during the physiological threshold series. By comparing neuronal thresholds measured under the two conditions, we aimed to determine whether the monkey's use of the visual stimulus influenced neuronal threshold. For both conditions thresholds were calculated using the procedure illustrated in Figure 5.

Figure 12 depicts the outcome of this comparison. For each neuron, the threshold measured in the "choice" condition (combined threshold series) is plotted against the threshold measured in the "fixation" condition (physiological threshold series). The two measurements were highly correlated (r = 0.85), and a paired t test revealed no difference between the logarithmically transformed thresholds obtained under the two conditions (p = 0.51). While we cannot completely rule out the possibility that the monkey continued to perform the discrimination covertly during the physiological threshold series, there was no overt sign

of decision-making activity such as eye movements to expected target locations. The thresholds of MT neurons therefore appear to be unaffected by the monkey's use of the visual stimulus. This result suggests that MT neurons faithfully encode the direction of motion in the stochastic display whether or not that information is currently of behavioral importance to the animal.

Discussion

We set out to determine the relative sensitivities of single cortical neurons and psychophysical observers to near-threshold motion signals. The surprising outcome is that the responses of a typical MT neuron can provide an accurate account of a monkey's psychophysical performance, including both the absolute position and the slope of the psychometric function relating performance to the strength of the motion signal. For half of the neurons in our study, the neurometric function derived from single-unit data was statistically indistinguishable from the psychometric function measured on the same set of trials. For most of the other neurons, the difference between neurometric and psychometric data could be attributed primarily to differences in threshold, although some neurometric functions differed in shape from the corresponding psychometric function. When neuronal and psychophysical thresholds differed, there was no consistent tendency for one or the other to be lower; when the slopes of the two functions differed, it was equally likely that the neuronal or psychophysical function would have the steeper slope. Thus, the distributions of threshold ratio and slope ratio illustrated in Figures 7 and 8 were both centered near unity.

It is important to be certain that this agreement is not artifactual. One possibility is that our chosen measurement time of 2 sec might inflate neuronal performance, but the analysis illustrated in Figure 11 shows that monkey and human observers integrate information over the full 2 sec viewing interval to reach decisions in our task. Another difficulty would arise if our monkeys were under imperfect behavioral control and were therefore performing at less than the best possible level, but we have presented in the Results our reasons for believing that our animals were fully trained and properly motivated throughout our experiments. A final possibility is that both neuronal and psychophysical performance was limited by the noise intrinsic to our stimulus, and not by neural computations. In most experiments the precise pattern of signal and noise dots was different on each trial, and the resulting variance might explain the variance in performance that is captured by the neurometric and psychometric functions. To explore the effects of this stimulus variance on neuronal response, we studied a subset of neurons under conditions in which precisely identical patterns of signal and noise dots were presented for each trial of a given stimulus condition. Were neuronal performance limited by the stimulus variance, we would expect a reduction in the variance of neuronal responses when stimulus variance is eliminated. In fact, this manipulation did not change neuronal response variance or indeed any other aspect of neuronal or psychophysical performance that we could measure (K. H. Britten, M. Shadlen, J. A. Movshon, and W. T. Newsome, unpublished observations). We therefore conclude that trial-to-trial variance in the visual stimulus had little or no influence on the results presented in this article.

Under our conditions, then, the performance of most neurons closely approximated the performance of the behaving monkey. This result is in contrast to a number of reports that individual neuron performance does not generally approach psychophys-
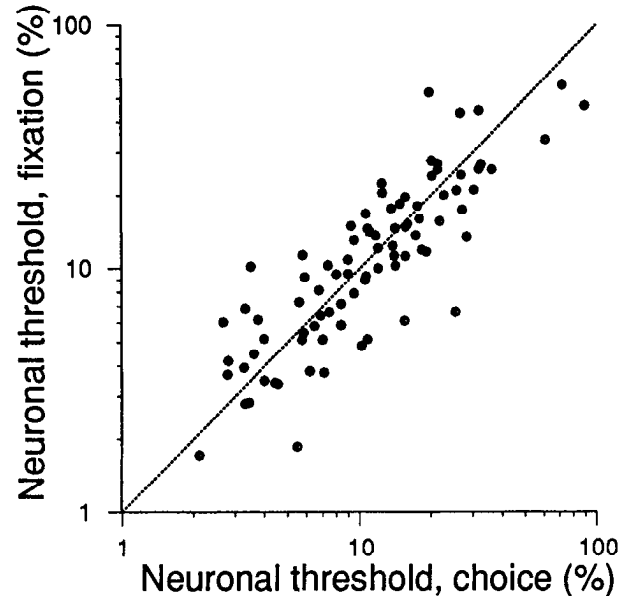

Figure 12. A comparison of neuronal thresholds measured in different behavioral states. The *abscissa* illustrates neuronal thresholds measured when the monkey was required to discriminate the direction of motion correctly in order to obtain a reward. The *ordinate* shows neuronal thresholds measured when the monkey was required only to fixate in order to obtain a reward. Both sets of data were obtained for 86 neurons in two monkeys. The *diagonal* is the line of unity slope; all data points would fall on this line if thresholds were identical in the two behavioral states.

ically measured levels. We believe that this apparent discrepancy is largely due to procedural differences between our study and earlier ones. In the present experiments, neuronal and psychophysical thresholds were measured under precisely identical conditions—in the same animal, on the same set of trials, and using the same visual stimuli. More importantly, we tailored the visual stimulus in each experiment to match the receptive field characteristics of the neuron under study—in eccentricity, size, preferred direction, and preferred speed. In most prior studies, neuronal thresholds were compared to psychophysical thresholds measured under very different conditions, frequently coming from different laboratories or different species. In the one case in which both sets of measurements were made in the same animal (Vogels and Orban, 1990), the psychophysical discrimination was not tailored to the receptive fields being studied. In the experiment whose results are most similar to ours, Hawken and Parker (1990) compared monkey neuronal and human psychophysical thresholds for contrast detection. They tailored the psychophysical stimuli to match the receptive fields of their neurons, and found a substantial minority of striate neurons whose performance roughly matched psychophysical performance under corresponding conditions. This suggests that much of the apparent discrepancy between our results and those of prior studies can be accounted for by a failure of previous studies to match stimulus conditions to receptive field properties. It is also likely, however, that genuine differences exist across perceptual tasks in the relation of neuronal to psychophysical sensitivity. Simple detection and discrimination tasks like those used in this study and by Hawken and Parker might well be based on small numbers of neural signals. Other more subtle or complex discriminations for which no reliable single neuron signals exist, however, are likely to create situations in which
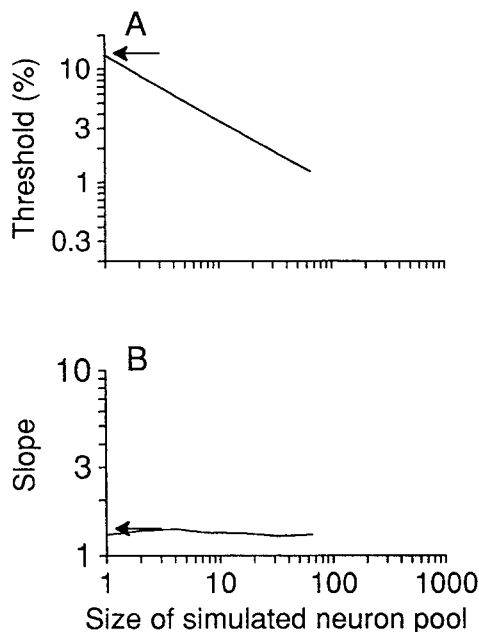
Figure 13. Simulated psychophysical performance for directional judgements based on the pooled responses of neurons recorded in this study. *A,* Simulated threshold as a function of pool size. The responses of neurons within each pool are assumed to be independent, and the output of a particular pool is the linear sum of the responses of the neurons in the pool. Data points in this and the following figures are geometric mean thresholds derived from a few thousand simulations. The *arrow* indicates the mean psychophysical threshold actually observed during our experiments. *B,* The slope of the simulated psychometric functions as a function of pool size. Data are from the same simulations illustrated in *A.* The *arrow* shows the mean psychometric function slope observed during our experiments.

no neuron approaches psychophysical performance levels. Informational demands vary substantially among psychophysical tasks, and it seems certain that organisms can adaptively pool the outputs of cortical neurons in different ways to meet those demands.

Under conditions like ours, we believe that the relationships between neurometric and psychometric data captured in Figures 7 and 8 are genuine. This implies that a monkey could perform the discrimination task with the observed sensitivity, were it capable of monitoring a single pair of MT cells in a neuron–antineuron configuration. This seems perplexing, because many directionally selective neurons in MT presumably carry signals relevant to the task, and it is not obvious why a monkey should be unable to take advantage of this pool of neurons to improve its psychophysical performance. Even if one assumes that only a small region of MT contains neurons whose receptive field properties are well matched in all respects to the demands of a particular task configuration, the number of available neurons might be on the order of hundreds if not thousands. To explore this issue, we conducted a series of simulations to learn how a monkey would perform were it able to pool signals from many neurons of the kind recorded during our study. The outcome of this exercise depends, of course, upon exactly which neurons are pooled and the manner in which their signals are combined, so we explored the effect of several different pooling rules on the simulated performance of neuronal populations of a plausible range of sizes.

Monte Carlo simulations. The details of our simulation procedure are described in the Appendix. On each trial, we simu-

lated the activity of a randomly chosen subset of the 216 neurons we studied by drawing randomly from synthetic response distributions based on analysis of the original neuronal data. We compiled these responses into separate "neuron" and "antineuron" pools, drawn respectively from the preferred direction and null direction response distributions, and used the difference between the pooled responses to determine a "decision" for each trial. By repeating this procedure for a suitable range of stimulus conditions, we simulated a complete psychophysical experiment. We then compiled the simulated decisions into psychometric functions, and fit them with smooth curves of the form given by Equation 1. In each simulation, we computed performance for pools containing from 1 to 1024 neurons; for each pool size, we generated several thousand psychometric functions, each based on a different random selection of cells from our sample of 216. We took the geometric mean of the slopes and thresholds derived from these functions to characterize the performance of the model for each set of conditions.

Our simulation procedure is based on the neuron–antineuron concept that we used to compute single neuron thresholds, in that it assumes that decisions in our task are based on a comparison of activity in two mechanisms with opposite preferred directions. Indeed, the simulation procedure reduces to the simple neuron–antineuron comparison when the pool contains one signal. For larger pool sizes, however, the simulation differs in that the comparison and the decision are effected only *after* signals from multiple neurons are pooled into larger aggregates.

Figure 13, *A* and *B,* shows the results of the simplest simulation, in which we calculated the pooled signals by summing the responses of the neurons in the pool; the decision on each trial was given to the pool with the larger response. The curve in Figure 13*A* shows that the mean simulated threshold fell dramatically as the neuron and antineuron pools were made larger. This improvement is expected because combining signals across multiple noisy sources permits more reliable discrimination of weak signals (Tolhurst et al., 1983; Watson, 1990, 1992). The arrow in Figure 13*A* shows the mean psychophysical threshold actually generated by our monkeys during these experiments. As expected, the agreement between simulated and observed performance is best for a pool size of one neuron. Here, the model should simulate our actual data analysis, and we know from Figure 7 that mean psychophysical threshold very nearly equals mean neuronal threshold. For pools as small as 16 neurons, simulated threshold falls to one-quarter of the observed value. The solid curve in Figure 13*B* shows that the mean simulated slope parameter remained roughly constant with increasing pool size. Furthermore, the simulated slopes agreed well with the mean slopes that characterized the monkeys' actual performance (arrow).

Because these simulations produce satisfactory agreement with our data only when the pool size is near 1, we could draw the simple conclusion that psychophysical performance in our paradigm must be based upon small numbers of neuronal signals. We must, however, explore three critical assumptions in the simulations: (1) *independence:* the responses of the neurons contributing to the pool are uncorrelated; (2) *linear summation:* the response of each pool is the sum of the responses of the constituent neurons; (3) *precision:* responses are counted and compared with absolute precision. Relaxing any of these assumptions importantly affects simulated performance, and we wished to determine how many neurons are required to account for observed performance as each assumption is relaxed.
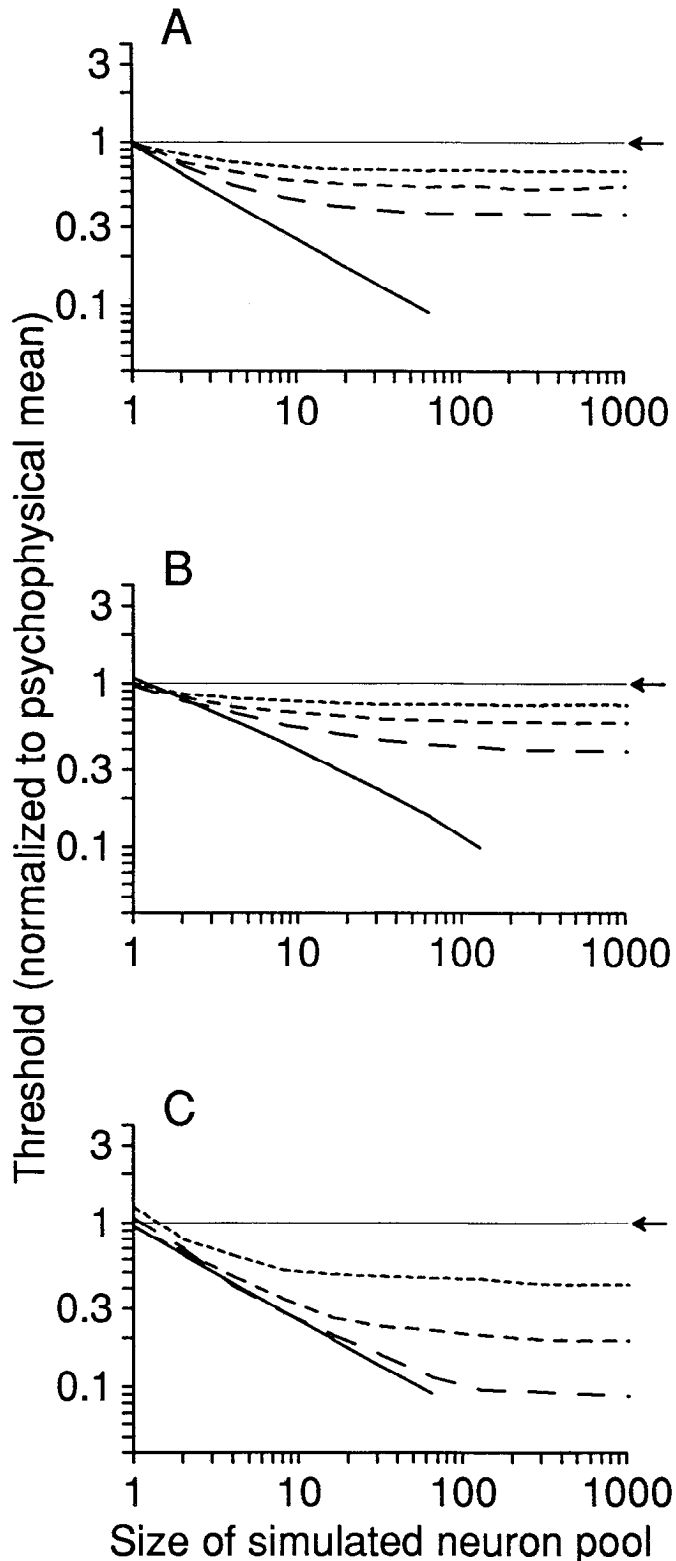
There are many reasons to believe that the assumption of statistical independence among neuronal responses is unreasonable. Nearby cortical neurons are richly interconnected and share many common inputs, and robust correlations among neuronal activity have been reported in a number of cortical areas (e.g., Gerstein et al., 1978; Abeles, 1982; Ts'o and Gilbert, 1988; Fetz et al., 1991). Figure 14*A* illustrates the performance of the model when the assumption of independence is relaxed. In this simulation, varying amounts of intercorrelation were imposed on all responses within each pool; no intercorrelation was introduced between the neuron and antineuron pools. In this and the remaining panels of Figure 14, the simulated thresholds are normalized to the average values obtained in our psychophysical experiments; an arrow and horizontal line mark the value of 1 at which the simulation's result would match the observed data. The bold solid line reproduces the performance expected for complete independence shown in Figure 13*A*. The broken lines show how performance changed as we introduced increasing amounts of correlated firing within the neuron and antineuron pools ($r = 0.25, 0.50,$ and 0.75). Increasing the degree of intercorrelation sharply diminishes the beneficial effect of pooling on performance. Intuitively, the simplest way to understand these effects is to recognize that intercorrelation among the members of a pool effectively reduces the number of independent signals in the pool, and correspondingly attenuates the effect of pool size. Inspection of the curves in Figure 14*A* shows that the intercorrelation we simulated imposes an asymptotic limit on performance, even as pool sizes grow very large. Inspection of the curves in Figure 14A shows that the intercorrelation we simulated imposes an asymptotic limit on performance. With an intercorrelation of 0.25, for example, arbitrarily large pool sizes yield simulated thresholds no lower than 36% of observed threshold. (Note that this same improvement can be obtained for pool sizes as small as four to six neurons if their responses are independent [solid curve]). Even with this asymptotic limit, simulated thresholds remain considerably lower than observed thresholds for reasonable levels of intercorrelation. Thus, small numbers of neurons still account best for observed performance unless an improbably high level of intercorrelation is postulated.

The idea that neuronal signals in a pool are summed linearly is also questionable. A number of psychophysical considerations (e.g., Pelli, 1985) suggest that larger signals make a disproportionate contribution to perceptual judgements, and we decided to simulate this by nonlinearly summing the responses of members of each pool. In this simulation, the pooled signal is computed as the square root of the sum of squared responses from each member of the pool; this is equivalent to the magnitude of the vector sum of orthogonal signals. The four curves in Figure 14*B* represent expected performance for the same set of intercorrelations used for Figure 14*A*, using this quadratic summation rule. This rule also attenuates the effect of pool size on threshold, but considerable improvement is still evident for modest pool sizes. The effect is to extend modestly the range of

Figure 14. Simulated psychophysical performance as a function of pool size, relaxing three important assumptions in the model. In each panel, the *horizontal line at 1.0* indicates the mean observed psychophysical threshold, to which all model thresholds were normalized. *A,* Simulated psychophysical thresholds assuming four different levels of correlated firing within the neuron and antineuron pools. The *solid line* reproduces simulated threshold for the no correlation condition, as illustrated in Figure 13*A*. The *broken lines, from bottom to top,* represent simulated threshold for increasing correlation coefficients: $r = 0.25$, $r = 0.50$, and $r = 0.75$. *B,* Simulated thresholds when responses are pooled

according to the square root summation rule. The curves illustrate the same four correlation levels employed in *A*. *C,* Simulated thresholds assuming varying levels of calculation imprecision. The *solid line* reproduces simulated performance shown in Figure 13*A* for perfect counting precision. *From bottom to top,* the *broken curves* illustrate simulated performance for increasing amounts of imprecision: $\epsilon = 0.04, 0.08,$ and 0.16.

Figure 15. Simulated performance when decisions are presumed to be influenced by neurons less sensitive than those recorded in the present study. *A,* Simulated thresholds based on the expanded data set including insensitive cells. Pooling and decision rules were identical to those employed in Figure 14*A.* The various curves illustrate different levels of response correlation, employing the same conventions as in Figure 14*A.* *B,* Slope of the simulated psychometric functions whose thresholds are illustrated in *A.* *C,* Simulated thresholds when less sensitive neurons are included in the data set *and* calculation imprecision is added. The various curves illustrate performance for different levels of imprecision as in Figure 14*C.* Responses are assumed to be independent, and pooling is by linear summation. *D,* Slope of the simulated psychometric functions whose thresholds are shown in *C.* Simulated thresholds were normalized as in Figure 14.
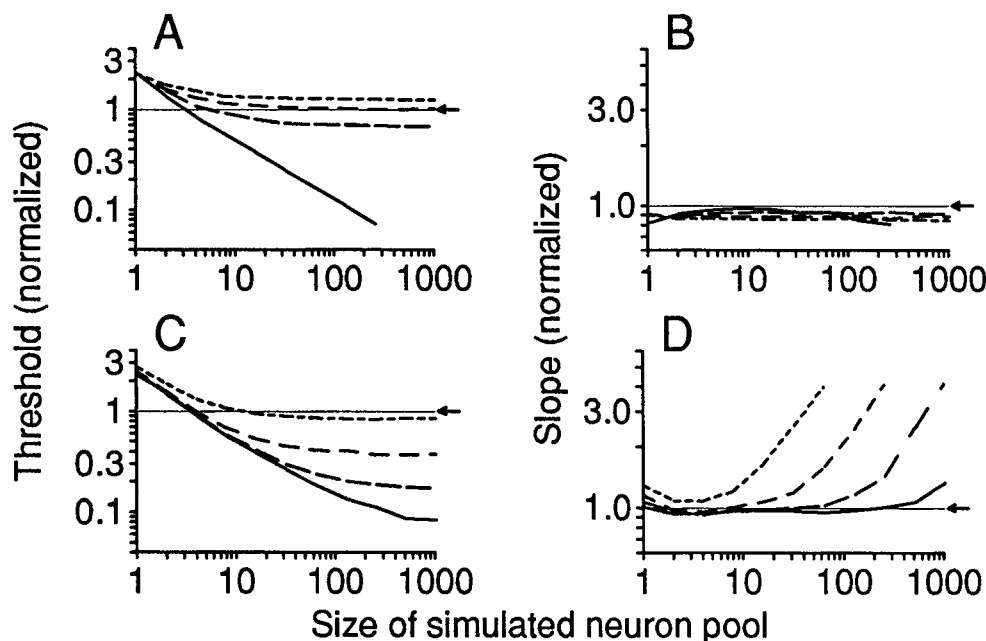
pool sizes compatible with observed psychophysical performance.

It might be argued that the monkey's cortex is less accurate at computing small differences between the activity of neurons or neuron pools than are our computers. Figure 14*C* explores the effect of relaxing the assumption of perfect computational accuracy. We suppose that the decision mechanism cannot count spikes precisely, and we therefore assume that decisions based on small differences between the activity of the neuron and antineuron pools are inherently unreliable. We simulated this unreliability by taking all cases in which a decision was based on a response difference less than a small proportion, ϵ, of the total response, and substituting a random "guess" for the computed decision. This has the effect of disrupting "low-confidence" decisions based on small differences between the responses of the two neuronal pools, but leaving unaffected "high-confidence" decisions based on large differences.

The effect of varying ϵ from 0 to 0.16 are explored in Figure 14*C.* For simplicity, only the conditions that linearly sum the responses of statistically independent neurons (as in Fig. 13) are shown. As expected, introducing imprecision elevates threshold slightly, and attenuates the effect of pool size on simulated threshold. The effect is generally similar to the effects of intercorrelation and nonlinear summation shown in Figure 14, *A* and *B,* and does not improve the agreement between our data and the simulated performance of large neuron pools. We therefore conclude that our model can tolerate modest amounts of calculation imprecision without requiring large neuronal pools to subserve performance.

The results of these simulations suggest that the inference of small pool size is quite robust with respect to the three assumptions outlined above. No substantial increase in the acceptable range of pool sizes can be gained by relaxing any of the three assumptions. Even if there were a high degree of correlation in the response variance of neurons within a pool, *and* if the individual responses were summed inefficiently, only pool sizes of approximately four to eight neurons are compatible with our observations (data not shown). Pools of this size remain

minute in comparison to the number of cortical neurons that carry signals of potential relevance to the task.

So far we have considered simulations based on the actual responses of our neurons. Recall that our measurements were all obtained under conditions in which the discrimination was optimized for the neuron under study. Our simulations therefore incorporate the assumption that performance is based *purely on the activity of neurons that prefer the particular direction, speed, and size of stimulus used.* However, suppose that other neurons, responding better to other stimuli, also contribute to perceptual judgement. The responses of these neurons would be less robust and reliable than those we have used until now, and might have a markedly deleterious effect on performance. To incorporate such neurons into our analysis, we simulated the inclusion of suboptimally activated neurons by randomly attenuating the responses of the neurons in the simulation to as little as 10% of the observed values (see Appendix for details). The value of 10% is arbitrary, but simulates the inclusion of neurons whose preferred directions might differ from the true direction by up to about 60°, or whose preferred speeds might differ by a factor of 5–10.

Figure 15*A* illustrates simulated thresholds when decisions are based on responses from this expanded sample of "cells," using pooling and decision rules otherwise identical to those in Figure 14*A,* in which signals of a controlled degree of intercorrelation are combined linearly. Notice that the simulated threshold for a one-neuron pool is now more than twice that actually observed. As pool size increases, simulated threshold declines toward the value observed in our experiments, with the best match between simulated and observed thresholds occurring for pool sizes near 4 when response variance is completely uncorrelated within a pool. When the pooled neurons are intercorrelated, threshold falls asymptotically until the pools grow to around 100 neurons. For suitable choices of intercorrelation (here, around 0.5), neuronal pools of essentially any size larger than 50 are compatible with our observations. Had we chosen a different distribution of random attenuations, then this asymptotic agreement would be obtained with a different level of

intercorrelation. It is possible that these simulated thresholds might be associated with unrealistic psychometric function shapes, but Figure 15B shows that the slopes of the simulated functions are unaffected by this manipulation.

Figure 15, C and D, shows the final simulation, in which we both expanded the neuron pool to include insensitive neurons and included the effects of calculation imprecision (as in Fig. 14C above). For high degrees of calculation imprecision, the simulated thresholds of large neuron pools are in good agreement with our data (Fig. 15C), but the slopes of the psychometric functions become too steep to be consistent (Fig. 15D). It must be noted that this steepening of the simulated psychometric function is a consequence of the particular way in which we conceive of calculation imprecision. Imprecision could also be modeled by the simple addition of noise to the signals that emerge from the pooling stage. The latter procedure raises threshold without changing slope, a pattern of effects that is essentially the same as that observed following incorporation of less sensitive neurons into the pools (see above). The data from this manipulation are therefore not shown.

The simulations in Figure 15 suggest that our findings can be made consistent with the use of large neuron pools if those pools include large numbers of neurons whose preferences poorly match the stimulus. Moreover, the inclusion of these neurons restricts our ability to relax the assumption of calculation precision, because under these circumstances large amounts of imprecision may cause the slope of the psychometric function to grow too steep.

Together, the simulation results in Figures 13–15 provide useful insights concerning the possible relationship of neuronal responses to psychophysical judgement. They allow us to define more precisely the conditions under which different-sized pools can plausibly account for the psychophysical data reported in this article. The hypothesis of a small pool size is most consistent with our data as long as decisions are based purely on optimally stimulated neurons. If suboptimally stimulated neurons are included, however, pools of essentially any size become compatible with observed psychophysical sensitivity, but *only* if the responses of the pooled neurons are partially correlated ($r = 0.25–0.75$; Fig. 15A,B) and if neuronal calculations are reasonably precise (Fig. 15C,D). Thus, our simulations indicate that a meaningful estimate of the number of neurons contributing signals to the decision process is critically dependent on the degree to which their responses are intercorrelated. This intercorrelation can be determined experimentally, and we have begun to make such measurements under conditions identical to those employed in the present study.

Perhaps the strongest conclusion permitted by our data is that psychophysical decisions in our paradigm depend upon a small number of independent neural *signals*, irrespective of pool size. If pool size is large and responses are partially correlated, the *effective* number of neural signals is small because the responses of the pooled neurons are largely redundant. If, on the other hand, responses are predominantly uncorrelated, performance is likely to depend upon a small number of signals carried by a correspondingly small number of neurons. Other observations made in this laboratory are consistent with this conclusion. For example, we have found that the responses of single neurons in MT can be reliably correlated with psychophysical decisions made by the monkey on a trial-to-trial basis, even when identical, near-threshold stimuli elicit the variable judgements (Britten et al., 1988; Newsome et al., 1989b). This rather startling

observation—that some portion of the variance in the psychophysical decision process is reflected in the response variance of single sensory neurons—is consistent with the conclusion that decisions are based on small numbers of neural signals. Interestingly, the phenomenon is neutral with respect to the issue of pool size: it is consistent with the hypothesis of small pools of independent neurons, but it is also present in our simulations of performance based on large pools of partially intercorrelated neurons. These data will be presented in detail in a forthcoming publication.

Concluding remarks. In an ongoing series of studies, we have employed a variety of techniques to investigate the role of visual area MT in mediating psychophysical judgements of motion direction. Lesion studies indicate that MT is necessary for optimal performance on our task (Newsome and Pare, 1988), the present single-unit study demonstrates that the information encoded by MT neurons is sufficient to account for psychophysical performance on the task, and microstimulation studies show that psychophysical judgements can be modified in a predictable manner by altering the activity of directional neurons in MT (Salzman et al., 1992). Together, these results demonstrate that neural signals in MT play an intimate role in a simple perceptual discrimination of motion direction. Ultimately, though, a complete neurophysiological account of performance on this task will require understanding how signals in MT are integrated with activity in areas upstream and downstream from MT. It is well known that MT is but one locus on a cortical pathway that appears specialized for motion analysis, and it is therefore likely that the exquisite sensitivity of MT neurons results from the convergence of signals from areas upstream to MT. It will be of interest to determine whether the sensitivity of those upstream neurons is similar to that of psychophysical observers when the demands of the task are matched to the properties of their individual receptive fields, or whether a close association between neuronal and psychophysical sensitivity emerges uniquely at the level of MT. Similarly, it will be interesting to determine whether microstimulation of upstream areas such as V1 and V3 can influence performance on the direction discrimination task.

In some ways, however, the most interesting questions lie downstream from MT. We have several times alluded to a "decision process" that evaluates the pooled signals emerging from "neuron" and "antineuron" channels in MT. We imagine the outcome of this evaluation to be a decision in favor of one or the other direction of motion, which may then inform the planning of an eye movement to the corresponding target LED. The decision process, in other words, is the link between the sensory representation of motion direction and the execution of a specific behavioral response. Decision processes are commonly invoked in cognitive psychology to link perception to action, and our behavioral paradigm provides a compact model system for physiological investigation of such a mechanism. We presume that the neural circuits of interest lie somewhere between the sensory representation of motion in MT and overtly oculomotor structures such as the superior colliculus and frontal eye fields. Current physiological and anatomical data suggest the cortex of the inferior parietal lobe as a likely locus for such circuits. The ascending outputs of MT are directed primarily toward the inferior parietal lobe (Maunsell and Van Essen, 1983a; Ungerleider and Desimone, 1986), and recent physiological data suggest that neurons in this region participate in the planning of intended eye movements (Gnadt and Anderson, 1988; Barash et

al., 1991; Duhamel et al., 1992). Learning the nature of neuronal signals in this cortex during performance of our task thus emerges as a particularly intriguing sequel to the present study.

Appendix

Here we describe the Monte Carlo methods used to simulate psychophysical performance from the responses of neurons like those we studied in MT. Performance was simulated for pool sizes ranging from 1 to 1024 neurons using several combinations of pooling and decision rules. For each pool size, N, we generated several thousand psychometric functions, each based on a random selection of N neurons from our data set of 216 cells. The geometric mean threshold and slope of these simulated functions provided estimates of the performance expected were decisions based on a pool of N neurons.

Basic procedure. Each iteration of the model, representing a single simulated "experiment," began with a new random selection of N cells (with replacement) and ended with a psychometric function parameterized by two constants reflecting threshold and slope, after Equation 1 above. During each iteration, we computed performance for 25 "trials" at each of 10 different motion strengths (correlation levels). On each trial, two responses were generated stochastically for each cell, one representing a response to preferred direction motion and the other representing a response to null direction motion. Preferred direction picks contributed to a "neuron" pool of responses, while null direction picks contributed to an "antineuron" pool. The antineuron pool is taken to represent the activity of an equivalent set of N cells whose preferred direction is opposite to that of the neuron pool. Responses were combined within each pool according to a specified summation rule. The summed responses of the two pools were then compared, and a judgement of motion direction was generated according to a specified decision rule. Following the logic of the neuron–antineuron model laid out above, a decision in favor of the preferred direction was scored as correct. Data from the 250 simulated trials were compiled into a psychometric function depicting the proportion of correct responses as a function of motion strength. The psychometric function was fitted with a curve of the form given by Equation 1 above (Quick, 1974; Watson, 1979), and the threshold and slope parameters were collected to complete the iteration.

Several thousand iterations were performed for each combination of pooling rule, decision rule, and pool size. The geometric mean of the thresholds thus derived provided a single data point in Figures 13A, 14, and 15, A and C. Similarly, the mean slope parameter provided a single data point in Figures 13B and 15, B and D. By varying the number of neurons contributing to each pool, we generated curves relating simulated psychophysical threshold (and slope) to pool size. For $N = 1$ neuron, the stochastic model generates mean performance equivalent to the means of our actual observations.

The curves depicting performance as a function of pool size in Figures 13–15 are affected systematically by the particular pooling and decision rules chosen as well as by assumptions concerning intercorrelation of responses within neuron pools and the precision of computations performed within the central nervous system.

Generation of neuronal responses. On each trial, the response of each cell in the pool was generated stochastically from the mean response and associated variance expected for that cell at the specified stimulus strength. The expected mean responses

and variances were based on actual physiological measurements made for each cell in the data base. The expected mean response of each neuron was determined from the best-fitting quadratic equation relating measured response to stimulus correlation (i.e., the correlation–response function):

$$\bar{x}_{\text{pref},i} = a_{0,i} + b_{\text{pref},i}\phi + c_{\text{pref},i}\phi^2$$

$$\bar{x}_{\text{null},i} = a_{0,i} + b_{\text{null},i}\phi + c_{\text{null},i}\phi^2, \qquad i = 1, \ldots, N, \quad \text{(A1)}$$

where ϕ represents motion strength (in percentage of correlated dots) and a, b, and c are fitted constants. Our physiological data are fitted well by such equations (Britten, Shadlen, Movshon, and Newsome, unpublished observations), and the resulting functions permit us to interpolate simulated responses to stimulus correlations not included during the actual physiological recordings. Separate fits were employed for motion in the preferred and null directions. Thus, for each neuron in our sample, an expected mean response could be calculated for any arbitrary stimulus correlation in either direction of motion.

For each mean response level, an associated response variance was calculated according to the power law

$$\sigma^2(\bar{x}) = .98\bar{x}^{1.26}, \quad \text{(A2)}$$

where $\bar{x}$ is the mean neuronal response. This law describes our data well under all stimulus conditions (Britten, Shadlen, Movshon, and Newsome, unpublished observations) and is similar to results obtained by other investigators (Dean, 1981; Tolhurst et al., 1983; Vogels et al., 1989).

In a separate set of simulations (Fig. 15), we modeled the effects of pooling among a larger population of neurons, including hypothesized cells that were less sensitive than those we recorded. To generate correlation–response functions for these less sensitive neurons, we assigned a random attenuation factor, G_i, uniformly distributed from 0.1 to 1, to each neuron. The hypothesized correlation–response functions for the two directions of motion are given by

$$\bar{x}_{\text{pref},i} = a_{\text{pref},i} + G_i(b_{\text{pref},i}\phi + c_{\text{pref},i}\phi^2),$$

$$\bar{x}_{\text{null},i} = a_{\text{null},i} + G_i(b_{\text{null},i}\phi + c_{\text{null},i}\phi^2), \quad i = 1, \ldots, N. \quad \text{(A3)}$$

A new attenuation factor was assigned to each neuron of the pool for each iteration of the model, that is, for each simulated psychometric function. Notice that the response to 0% correlation is not affected by the attenuation factor. Rather, it is the slope, or gain, of the correlation–response function that is modified. Figure 15 illustrates simulations for random attenuation factors in the range of from 0.1 to 1. This procedure permits us to estimate performance as a function of pool size for pools that include neurons less sensitive than those we recorded.

Correlation. We have no actual measurements of the degree of intercorrelation between the responses of MT neurons. Rather, response correlation was incorporated as a model assumption by forcing the stochastic responses from each of the N neurons within a pool to conform to a specified correlation coefficient, r (0, 0.25, 0.5, or 0.75). Thus, the specified correlation coefficient would capture the relationship displayed in a scatterplot of the responses of any pair of neurons in the pool. To impose this correlation in our simulations, we modified a standard numerical recipe for generating Poisson deviates so that responses could be generated randomly for each neuron, reflecting the

expected mean responses and associated variances as well as the specified intercorrelation.

In the absence of correlation ($r = 0$), the response of a cell on a given trial is a random value drawn from a scaled Poisson distribution of the expected mean and variance. Let $X_i(\bar{x}_i, \sigma_i^2)$ represent a random variable with probability density approximating the response distribution of the ith neuron. A random value from this distribution, denoted x_i, is well approximated by multiplication of a constant times a Poisson deviate with mean and variance, μ:

$$x_i = \alpha \text{ Poidev}(\mu), \qquad \text{(A4)}$$

where

$$\mu = \bar{x}_i^2/\sigma_i^2, \qquad \alpha\mu = \bar{x}_i. \qquad \text{(A5)}$$

We employed a routine for generating Poisson deviates described by Press et al. (1988).

In addition, we required that the picks from any pair of neurons possess the correlation coefficient, r. This was accomplished by generating random picks for each neuron, conditional upon the deviates of a common random dummy variable, $Y(\bar{y}, \sigma_d^2)$ such that the correlation coefficient between each neuron, X_i, and Y is

$$\rho_{i,d} = \sqrt{r}. \qquad \text{(A6)}$$

For normally distributed random variables, these conditional distributions may be constructed as independent distributions with revised mean and variance:

$$X_i(\bar{x}_i, \sigma_i^2 \mid y) = X_i(m_i, s_i^2), \qquad \text{(A7)}$$

where

$$m_i = \bar{x}_i + \rho_{i,d}(\sigma_i/\sigma_d)(y - \bar{y}) \qquad \text{(A8)}$$

and

$$s_i^2 = \sigma_i^2(1 - \rho_{i,d}^2). \qquad \text{(A9)}$$

These relationships follow from the regression of X on Y. Notice that the conditional picks from each neuron are generated independently, so the conditional covariance is zero. Again, for normally distributed random variables, it can be shown that the actual (nonconditional) correlation coefficient between any pair of random variables $X_{i \neq j}$ is

$$\rho_{i,j} = \rho_{i,d}^2 = r. \qquad \text{(A10)}$$

These relationships are proven for the normal case by Anderson (1958). It is natural to expect the more physiologically plausible scaled Poisson distributions to inherit these properties, and we have verified this numerically. The standard deviation of $\rho_{i,j}$ is approximately 0.1 for $r = 0$, and shrinks to 0.04 for $r = 0.75$.

Equations A4–A10 provide an algorithm for generating partially correlated random deviates from physiologically plausible distributions of known mean and variance. It is a convenient approach since it allows us to covary as many processes as needed by referencing a common pick from the dummy variable, Y, and calling a standard numerical recipe for computing Poisson deviates. We employed this method to generate partially correlated response values from multiple neurons in the simulations illustrated in Figures 14, *A* and *B*, and 15, *A* and *B*.

For each simulation, the same correlation coefficient, r, was imposed on the responses within "neuron" and "antineuron" pools. Since the neuron and antineuron pools are intended to represent separate and opposing pools of neurons, we imposed no correlation *between* the two pools.

Pooling. On each trial, responses were generated stochastically from preferred direction response distributions of N cells to form the "neuron" pool, and responses were generated from the null direction distributions of the same N cells to form the "antineuron" pool. These responses were combined within the two pools to generate a single pair of values upon which the psychophysical "decision" was based. The manner in which signals are combined within the nervous system is not known and was therefore incorporated as a model assumption. We used either the linear sum of N signals,

$$R_{\text{pref}} = \sum_{i=1}^{N} x_{\text{pref},i}, \qquad R_{\text{null}} = \sum_{i=1}^{N} x_{\text{null},i}, \qquad \text{(A11)}$$

or the magnitude of their vector sum, assuming mutual orthogonality,

$$R_{\text{pref}} = \left[\sum_{i=1}^{N} x_{\text{pref},i}^2\right]^{1/2}, \qquad R_{\text{null}} = \left[\sum_{i=1}^{N} x_{\text{null},i}^2\right]^{1/2}. \qquad \text{(A12)}$$

The latter may be recognized as the expected sum of uncorrelated random signals. Here, the term "uncorrelated" would refer to the temporal structure of the neural discharge, rather than its amplitude (number of spikes). It is possible for several neurons to be highly correlated in their total response and yet possess little correlation in the temporal structure of their discharge. A linear mechanism might be expected to add these signals as orthogonal vectors.

We have also modeled nonlinear summation rules of the form

$$R_{\text{pref}} = \left[\sum_{i=1}^{N} x_{\text{pref},i}^k\right]^{-1/k}, \qquad R_{\text{null}} = \left[\sum_{i=1}^{N} x_{\text{null},i}^k\right]^{-1/k}, \qquad k > 2. \qquad \text{(A13)}$$

Less efficient summation occurred as k increased, with rapid convergence to a winner-take-all rule in which the pooled responses were dominated by the pair of neurons yielding the largest responses to preferred and null direction motion, respectively.

Decision. On each trial, the pooled responses to opposing directions of motion were compared, and a psychophysical decision was rendered. The decision rule was to choose the direction of motion favored by the pool that yielded the largest response:

$$R_{\text{pref}} > R_{\text{null}}, \qquad \text{choose PREF,}$$

$$R_{\text{null}} > R_{\text{pref}}, \qquad \text{choose NULL,}$$

$$R_{\text{pref}} = R_{\text{null}}, \qquad \text{GUESS.} \qquad \text{(A14)}$$

During actual psychophysical experiments, the direction of motion varied randomly from trial to trial so that the monkey had no basis for anticipating the correct answer. Such precautions are unnecessary for modeling purposes, and we therefore pretended that motion was always in the preferred direction. Therefore a preferred decision was always correct, and a null decision was always incorrect. A guess had 50% probability of being correct, but this condition had little impact on the simulations

since the neuron and antineuron pools rarely yielded identical responses.

Computational imprecision may be incorporated into the model by requiring that the difference between the pooled signals exceed some specified margin before a decision can be reliably projected. The decision rule thus becomes

$$R_{pref} > R_{null} + \delta, \quad \text{choose PREF,}$$

$$R_{null} > R_{pref} + \delta, \quad \text{choose NULL,}$$

$$|R_{pref} - R_{null}| \leq \delta, \quad \text{GUESS,} \quad (A15)$$

where δ is the margin of imprecision. It is sensible to model this quantity as a fraction of the pooled signal,

$$\delta = \epsilon \, Max(R_{pref}, R_{null}), \quad 0 \leq \epsilon \leq 1. \quad (A16)$$

In order for a reliable decision to ensue, the larger of the pooled signals representing opposing directions must exceed the smaller by some fraction, ϵ. This is a simple realization of the notion that the neural processes within the monkey's visual system may be unable to count spikes with the accuracy of a digital computer. Physiologically, such imprecision may be thought of as the consequence of summing pooled responses with a leaky integrator. We allowed ϵ to vary from 0% to 16% (see Figs. 14, 15).

We also examined an alternative model for decision imprecision by simply adding zero-mean noise to the pooled response values. This procedure is equivalent to incorporating unusually variable neurons in the pooled response, and its effects are therefore approximated by the simulations employing randomly attenuated neural sensitivities.

References

Abeles M (1982) Local cortical circuits. Berlin: Springer.

Albright TD (1984) Direction and orientation selectivity of neurons in visual area MT of the macaque. J Neurophysiol 52:1106–1130.

Allman JM, Kaas JH (1971) A representation of the visual field in the caudal third of the middle temporal gyrus of the owl monkey (Aotus trivirgatus). Brain Res 31:85–105.

Allman JM, Meizen F, McGuinness E (1985a) Stimulus specific responses from beyond the classical receptive field: neurophysiological mechanisms for local-global comparisons in visual neurons. Annu Rev Neurosci 8:407–430.

Allman JM, Meizin F, McGuinness E (1985b) Direction and velocity-specific responses from beyond the classical receptive field in the middle temporal visual area (MT). Perception 14:105–126.

Anderson T (1958) An introduction to multivariate statistical analysis, pp 27–34. New York: Wiley.

Baker JF, Petersen SE, Newsome WT, Allman JM (1981) Visual response properties of neurons in four extrastriate visual areas of the owl monkey (Aotus trivirgatus). J Neurophysiol 45:397–416.

Ball K, Sekuler R (1982) A specific and enduring improvement in visual motion discrimination. Science 218:697–698.

Ball K, Sekuler R (1987) Direction-specific improvement in motion discrimination. Vision Res 27:953–965.

Bamber D (1975) The area above the ordinal dominance graph, the area below the receiver operating characteristic graph. J Math Psychol 12:387–415.

Barash S, Bracewell RM, Fogassi L, Gnadt JW, Andersen RA (1991) Saccade-related activity in the lateral intraparietal area: I. Temporal properties; comparison with area 7a. J Neurophysiol 66:1095–1108.

Barlow H (1972) Single units, sensation: a neuron doctrine for perceptual psychology? Perception 1:371–394.

Barlow HB, Levick WR, Yoon M (1971) Responses to single quanta of light in retinal ganglion cells of the cat. Vision Res [Suppl] 3:87–101.

Barlow HB, Kaushal TP, Hawken M, Parker AJ (1987) Human contrast discrimination and the threshold of cortical neurons. J Opt Soc Am A 4:2366–2371.

Bradley A, Skottun BC, Ohzawa I, Sclar G, Freeman RD (1987) Visual orientation and spatial frequency discrimination: a comparison of single cells and behavior. J Neurophysiol 57:755–772.

Britten KH, Newsome WT, Movshon JA (1988) Association between cortical unit activity and psychophysical response in alert monkeys. Soc Neurosci Abstr 14:458.

Cohn TE, Green DG, Tanner WP (1971) Receiver operating characteristic analysis. Application to the study of quantum fluctuation in optic nerve of Rana pipiens. J Gen Physiol 66:583–616.

Cowey A, Weiskrantz L (1968) Varying spatial separation of cues, response, and reward in visual discrimination learning in monkeys. J Comp Physiol Psychol 11:220–224.

Crist CF, Yamasaki DSG, Komatsu H, Wurtz RH (1988) A grid system and a microsyringe for single cell recording. J Neurosci Methods 26:117–122.

Dean AF (1981) The variability of discharge of simple cells in cat striate cortex. Exp Brain Res 44:437–440.

Downing CJ, Movshon JA (1989) Spatial and temporal summation in the detection of motion in stochastic random dot displays. Invest Ophthalmol Vis Sci [Suppl] 30:72.

Dubner R, Zeki SM (1971) Response properties and receptive fields of cells in an anatomically defined region of the superior temporal sulcus. Brain Res 35:528–532.

Duhamel J-R, Colby CL, Goldberg ME (1992) The updating of the representation of visual space in parietal cortex by intended eye movements. Science 255:1–32.

Evarts EV (1966) A technique for recording activity of subcortical neurons in moving animals. Electroencephalogr Clin Neurophysiol 24:83–86.

Fetz E, Toyama K, Smith W (1991) Synaptic interactions between cortical neurons. In: Cerebral cortex (Peters A, Jones EG, eds), pp 1–47. New York: Plenum.

Gallyas F (1979) Silver staining of myelin by means of physical development. Neurol Res 1:203–209.

Gerstein GL, Perkel DH, Subramian KN (1978) Identification of functionally related neural assemblies. Brain Res 140:43–62.

Gnadt JW, Andersen RA (1988) Memory related motor planning activity in posterior parietal cortex of monkey. Exp Brain Res 70:216–220.

Green DM, Swets JA (1966) Signal detection theory and psychophysics. New York: Wiley.

Hawken MJ, Parker AJ (1990) Detection and discrimination mechanisms in the striate cortex of the old-world monkey. In: Vision: coding and efficiency (Blakemore C, ed), pp 103–116. Cambridge: Cambridge UP.

Hays AV, Richmond BJ, Optican LM (1982) A UNIX-based multiple process system for real-time data acquisition and control. WESCON Conf Proc 2:1–10.

Hoel P, Port S, Stone C (1971) Introduction to statistical theory, p 83ff. Boston: Houghton Mifflin.

Johnson N, Kotz S (1969) Discrete distributions. New York: Wiley.

Judge SJ, Richmond BJ, Chu FC (1980) Implantation of magnetic search coils for measurement of eye position: an improved method. Vision Res 20:535–538.

Lettvin JY, Maturana HR, McCulloch WS, Pitts WH (1959) What the frog's eye tells the frog's brain. Proc Inst Rad Eng 47:1940–1951.

Maunsell JHR, Van Essen DC (1983a) The connections of the middle temporal visual area (MT) and their relationship to a cortical hierarchy in the macaque monkey. J Neurosci 3:2563–2586.

Maunsell JHR, Van Essen DC (1983b) Functional properties of neurons in the middle temporal visual area (MT) of the macaque monkey: I. Selectivity for stimulus direction, speed and orientation. J Neurophysiol 49:1127–1147.

Merigan WH (1980) Temporal modulation sensitivity of macaque monkeys. Vision Res 20:953–959.

Mishkin M, Weiskrantz L (1958) Effects of delaying reward on visual discrimination learning with frontal lesions. J Comp Physiol Psychol 3:276–281.

Morgan MJ, Ward R (1980) Conditions for motion flow in dynamic visual noise. Vision Res 20:431–435.

Newsome WT, Pare EB (1988) A selective impairment of motion perception following lesions of the middle temporal visual area (MT). J Neurosci 8:2201–2211.

Newsome WT, Britten KH, Movshon JA (1989a) Neuronal correlates of a perceptual decision. Nature 341:52–54.

Newsome WT, Britten KH, Movshon JA, Shadlen M (1989b) Single

neurons and the perception of visual motion. In: Proceedings of the retina research foundation, Neural mechanisms of visual perception, vol 2 (Lam DM-K, Gilbert CD, eds), pp 171–198. The Woodlands, TX: Portfolio.

Newsome WT, Britten KH, Salzman CD, Movshon JA (1990) Neuronal mechanisms of motion perception. Cold Spring Harbor Symp Quant Biol 55:697–705.

Parker A, Hawken M (1985) Capabilities of monkey cortical cells in spatial-resolution tasks. J Opt Soc Am A 2:1101–1114.

Pasternak T, Horn KM, Maunsell JHR (1989) Deficits in speed discrimination following lesions of the lateral suprasylvian cortex in the cat. Vis Neurosci 3:365–375.

Pelli DG (1985) Uncertainty explains many aspects of visual contrast detection and discrimination. J Opt Soc Am A 2:1508–1531.

Pirenne MH (1943) Binocular and uniocular threshold of vision. Nature 152:698–699.

Press WH, Flannery BP, Teukolsky SA, Vetterling WT (1988) Numerical recipes in C, pp 221–223. Cambridge, MA: Cambridge UP.

Quick RF (1974) A vector magnitude model of contrast detection. Kybernetik 16:65–67.

Salzman CD, Britten KH, Newsome WT (1990) Cortical microstimulation influences perceptual judgements of motion direction. Nature 346:174–177.

Salzman CD, Murasugi CM, Britten KH, Newsome WT (1992) Microstimulation in visual area MT: effects on direction discrimination performance. J Neurosci 12:2331–2356.

Tolhurst DJ, Movshon JA, Dean AF (1983) The statistical reliability of signals in single neurons in cat and monkey visual cortex. Vision Res 23:775–785.

Ts'o DY, Gilbert CD (1988) The organization of chromatic and spatial interactions in the primate striate cortex. J Neurosci 8:1712–1727.

Ungerleider LG, Desimone R (1986) Cortical connections of visual area MT in the macaque. J Comp Neurol 248:190–222.

Ungerleider LG, Mishkin M (1979) The striate projection in the superior temporal sulcus of *Macaca mulatta*: location and topographic organization. J Comp Neurol 188:347–366.

Van Essen DC, Maunsell JHR, Bixby JL (1981) The middle temporal visual area in the macaque: myeloarchitecture, connections, functional properties and topographic representation. J Comp Neurol 199: 293–326.

Vogels R, Orban GA (1990) How well do response changes of striate neurons signal differences in orientation: a study in the discriminating monkey. J Neurosci 10:3543–3558.

Vogels R, Spileers W, Orban GA (1989) The response variability of striate cortical neurons in the behaving monkey. Exp Brain Res 77: 432–436.

Watson AB (1979) Probability summation over time. Vision Res 19: 515–522.

Watson AB (1990) Gain, noise, contrast sensitivity of linear visual neurons. Visual Neurosci 4:147–157.

Watson AB (1992) Transfer of contrast sensitivity in linear visual networks. Visual Neurosci 8:65–76.

Werner G, Mountcastle VB (1963) The variability of central neural activity in a sensory system, and its implications for the central reflection of sensory events. J Neurophysiol 26:958–977.

Zeki SM (1974) Functional organization of a visual area in the posterior bank of the superior temporal sulcus of the rhesus monkey. J Physiol (Lond) 236:549–573.

Zohary E (1992) Population coding of visual stimuli by cortical neurons tuned to more than one dimension. Biol Cybern 66:265–272.